# N-Heterocyclic Donor- and Acceptor-Type Ligands Based on 2-(1H-[1,2,3]Triazol-4-yl)pyridines and Their Ruthenium(II) Complexes

Bobby Happ,[†,‡] Daniel Escudero,[§] Martin D. Hager,[†,‡] Christian Friebe,[†] Andreas Winter,[†,‡,⊥] Helmar Görls,[¶] Esra Altuntaş,[†] Leticia González,*[,§] and Ulrich S. Schubert*[,†,‡,⊥]

[†]*Laboratory of Organic and Macromolecular Chemistry, Friedrich-Schiller-University Jena, Humboldtstrasse 10, 07743 Jena, Germany,* [‡]*Dutch Polymer Institute (DPI), P.O. Box 902, 5600 AX Eindhoven, The Netherlands,* [§]*Laboratory of Physical Chemistry, Friedrich-Schiller-University Jena, Helmholtzweg 4, 07743 Jena, Germany,* [⊥]*Laboratory of Macromolecular Chemistry and Nanoscience, Eindhoven University of Technology, P.O. Box 513, 5600 MB Eindhoven, The Netherlands, and* [¶]*Laboratory of Inorganic and Analytical Chemistry, Friedrich-Schiller-University Jena, Lessingstrasse 8, 07743 Jena, Germany*

To whom correspondence should be addressed. L.G.: fax +49 (0)3641 948302 and e-mail leticia. gonzalez@uni-jena.de. U.S.S.: fax: +49 (0)3641 948202, e-mail ulrich.schubert@uni-jena.de, and internet www.schubert-group.com.

Received February 19, 2010
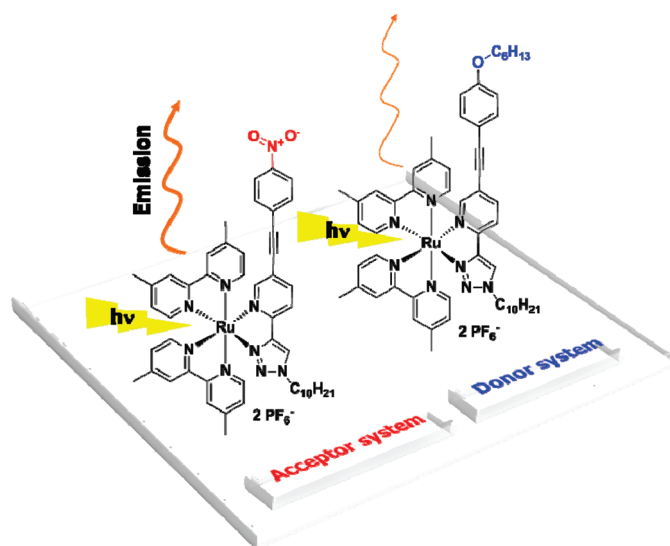
New 2-(1H-[1,2,3]triazol-4-yl)pyridine bidentate ligands were synthesized as bipyridine analogs, whereas different phenylacetylene moieties of donor and acceptor nature were attached at the 5-position of the pyridine unit. The latter moieties featured a crucial influence on the electronic properties of those ligands. The N-heterocyclic ligands were coordinated to ruthenium(II) metal ions by using a bis(4,4'-dimethyl-2,2'-bipyridine)ruthenium(II) precursor. The donor or acceptor capability of the 2-(1H-[1,2,3]triazol-4-yl)pyridine ligands determined the quantum yield of the resulting ruthenium(II) complexes remarkably. Separately, 2-([1,2,3]triazol-4-yl)pyridine ligands are known to be potential quenchers, but using these new ligand systems led to room temperature emission of the corresponding ruthenium(II) complexes. The compounds have been fully characterized by elemental analysis, high-resolution ESI mass spectrometry, ^{1}H and ^{13}C NMR spectroscopy, and X-ray crystallography. Theoretical calculations for two ruthenium(II) complexes bearing a donor and acceptor unit, respectively, were performed to gain a deeper understanding of the photophysical behavior.

Introduction

The well-known N-heterocycles 2,2'-bipyridine (bpy) and 2,2':6',2''-terpyridine (tpy) have been widely studied owing to their predictable coordination behavior and the interesting photophysical and electrochemical properties that can result from their corresponding metal complexes. Such distinctiveness can be utilized for supramolecular self-assembly, molecular electronics, and catalysis applications.[1] Because functionalization

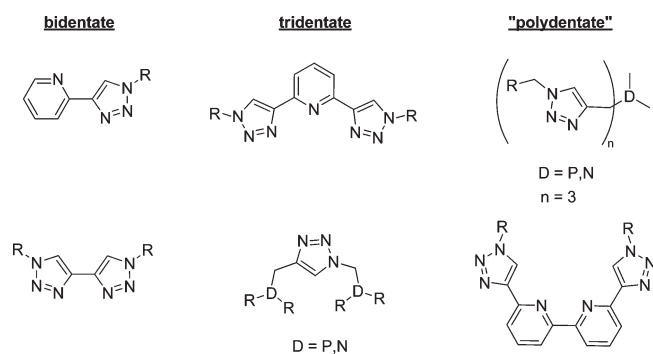**bidentate**   **tridentate**   **"polydentate"**

FIGURE 1. Schematic representation of 1*H*-[1,2,3]triazole-containing ligand architectures.

of polypyridine-based chelators can be synthetically troublesome,[2] it remains important to search for new approaches in the preparation of analogous bidentate chelating ligands that also possess well-defined coordination properties and can be prepared and modified with high effectiveness. In this respect the Cu[I]-catalyzed 1,3-cycloaddition of organic azides with terminal alkynes (the CuAAC reaction) has a great potential due to its mild reaction conditions and wide range of usable substrates.[3] The latter features have directed its application in the synthesis of functional molecules for biological and material sciences.[4] Furthermore, the development of the CuAAC reaction resulted in an increased interest toward the coordination chemistry of 1,4-functionalized 1*H*-[1,2,3]triazoles due to their potential as *N*-donor ligands. A variety of new bi-,[5,6] tri-,[7] and polydentate[6] 1*H*-[1,2,3]-triazole-containing ligands have been synthesized and their coordination properties were investigated (Figure 1).

Our interest was to tune in particular the electronic properties of the bidentate 2-(1*H*-[1,2,3]triazol-4-yl)pyridine ligands. This was accomplished by introducing electron-donating and electron-withdrawing units on the 5-position of the pyridine ring with a 2-(1*H*-[1,2,3]triazol-4-yl)pyridine system (trzpy) as central structural motive (Scheme 1). In the present study the synthesis and the characterization of new 2-(1*H*-[1,2,3]triazol-4-yl)pyridine ligand systems with donor and acceptor nature are described by using the efficient Sonogashira coupling and the versatile copper(I)-catalyzed azide–alkyne 1,3-cycloaddition intended for the ligand synthesis as well as the subsequent coordination onto a bis-(4,4′-dimethyl-2,2′-bipyridine)ruthenium(II) precursor complex. The photophysical properties were studied by UV-vis and emission spectroscopy, cyclic voltammetry and analyzed in detail by theoretical calculations.

The coordination to the ruthenium(II) metal ion by using bis(4,4′-dimethyl-2,2′-bipyridine) as ancillary ligand revealed two interesting features. First, 2-(1*H*-[1,2,3]triazol-4-yl)-pyridine systems are known to be potential luminescence quenchers at room temperature as soon as they are attached to a ruthenium(II) metal ion[8] and, unexpectedly, the herein described heteroleptic ruthenium(II) complexes bearing a 2-(1*H*-[1,2,3]triazol-4-yl)pyridine ligand furnished with an acceptor unit overcame this luminescence quenching and yielded in room temperature emission. Second, by replacing the latter acceptor system with a donor structure the luminescence at room temperature decreased considerably. Therefore, time-dependent density functional theory calculations (TD-DFT) were done to gain a deeper insight into the photophysical processes.
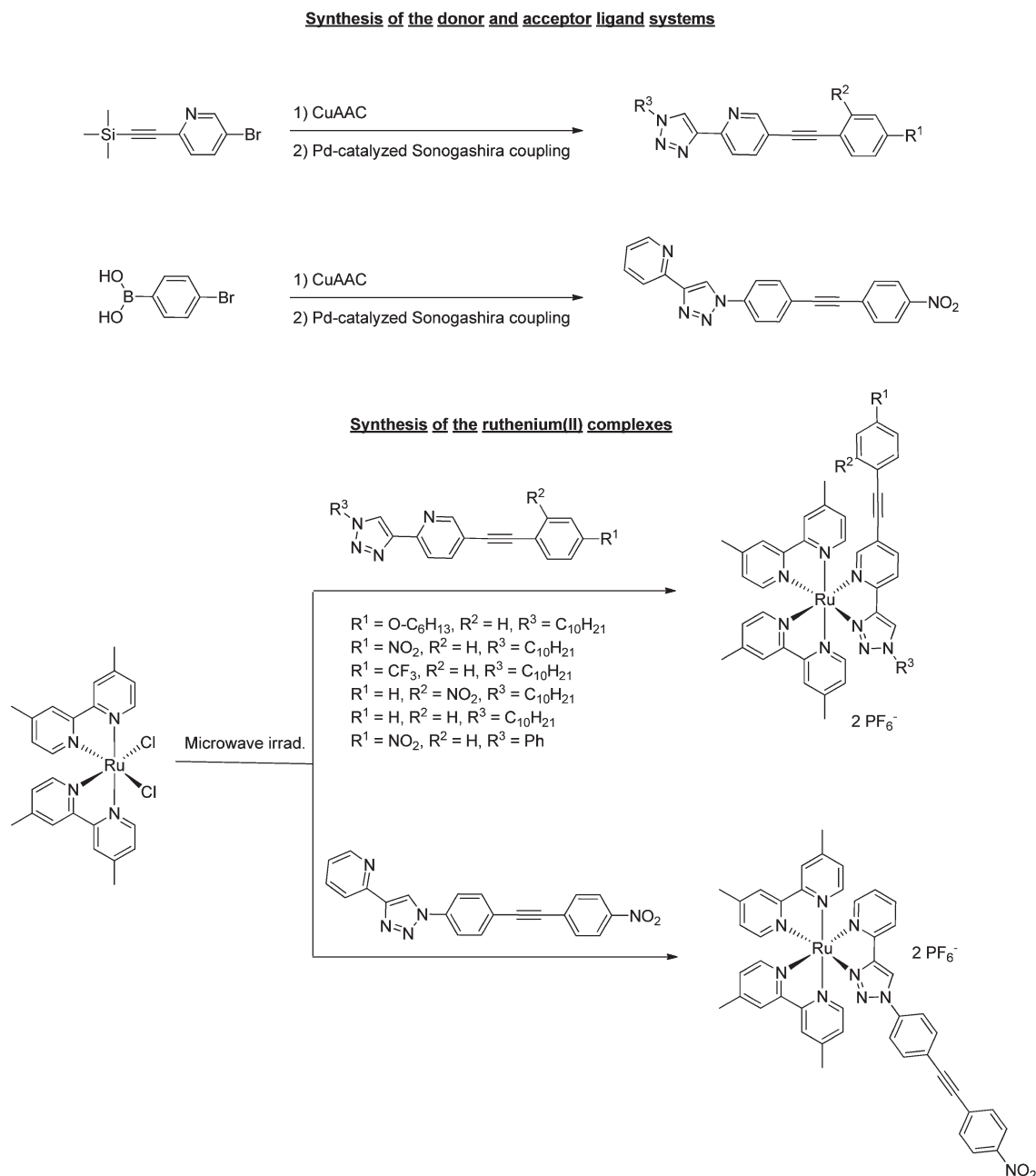
Results and Discussion

Synthesis. The general procedure for the synthesis of donor-type 2-(1*H*-[1,2,3]triazol-4-yl)pyridine **5** is outlined in Scheme 2. The Sonogashira cross-coupling[9] and the CuAAC[3b,c] reaction were the key reaction types for the construction of the targeted ligand. Consecutive Sonogashira reactions with 2 mol % of Pd[0] catalyst were carried out to synthesize intermediate **3**. Subsequently, deprotection of the trimethylsilyl group (TMS) utilizing fluoride ions afforded **4** in good yield (75%). The subsequent CuAAC reaction provided the final product **5** (67% yield) by using 5 mol % CuSO$_4$ and 25 mol % sodium ascorbate as the catalytic system. The purity of **5** was proven by NMR spectroscopy, mass spectrometry, and elemental analysis.

The synthesis of the acceptor systems **10a–d** also involved the Sonogashira cross-coupling and the CuAAC reaction as synthetic tools; however, a different synthetic approach had to be used. The synthesis of a precursor compound similar to **3** with electron-withdrawing substituents could not be performed. As a result, two alternative routes were applied to synthesize precursor compound **9** (Scheme 3). Though the first route consisted of one step less, both routes gave comparable overall yields (route 1: 61%; route 2: 51%). The reason for this observation might be the efficient cleavage of the TMS group[10] affording **6**

(1) (a) Balzani, V.; Juris, A.; Venturi, M.; Campagna, S.; Serroni, S. *Chem. Rev.* **1996**, *96*, 759–833. (b) Schubert, U. S.; Eschbaumer, C. *Angew. Chem., Int. Ed.* **2002**, *41*, 2892–2926. (c) Hofmeier, H.; Schubert, U. S. *Chem. Soc. Rev.* **2004**, *33*, 373–399. (d) Sauvage, J.-P.; Collin, J.-P.; Chambron, J.-C.; Guillerez, S.; Coudret, C. *Chem. Rev.* **1994**, *94*, 993–1019. (e) Amabilino, D. B.; Stoddart, J. F. *Chem. Rev.* **1995**, *95*, 2725–2828.

(2) (a) Newkome, G. R.; Patri, A. K.; Holder, E.; Schubert, U. S. *Eur. J. Org. Chem.* **2004**, 235–254. (b) Heller, M.; Schubert, U. S. *Eur. J. Org. Chem.* **2003**, 947–961. (c) Marin, V.; Holder, E.; Schubert, U. S. *J. Polym. Sci., Part A: Polym. Chem.* **2004**, *42*, 374–385.

(3) (a) Kolb, H. C.; Finn, M. G.; Sharpless, K. B. *Angew. Chem., Int. Ed.* **2001**, *40*, 2004–2021. (b) Tornoe, C. W.; Christensen, C.; Meldal, M. *J. Org. Chem.* **2002**, *67*, 3057–3064. (c) Rostovtsev, V. V.; Green, L. G.; Fokin, V. V.; Sharpless, K. B. *Angew. Chem., Int. Ed.* **2002**, *41*, 2596–2599.

(4) (a) Lutz, J.-F. *Angew. Chem., Int. Ed.* **2007**, *46*, 1018–1025. (b) Bock, V. D.; Hiemstra, H.; van Maarseveen, J. H. *Eur. J. Org. Chem.* **2005**, 51–68. (c) Meldal, M.; Tornoe, C. W. *Chem. Rev.* **2008**, *108*, 2952–3015. (d) Kolb, H. C.; Sharpless, K. B. *Drug Discovery Today* **2003**, *8*, 1128–1137. (e) Angell, Y. L.; Burgess, K. *Chem. Soc. Rev.* **2007**, *36*, 1674–1689. (f) Becer, C. R.; Hoogenboom, R.; Schubert, U. S. *Angew. Chem., Int. Ed.* **2009**, *48*, 4900–4908.

(5) (a) Schweinfurth, D.; Hardcastle, K. I.; Bunz, U. H. F. *Chem. Commun.* **2008**, 2203–2205. (b) Monkowius, U.; Ritter, S.; Koenig, B.; Zabel, M.; Yersin, H. *Eur. J. Inorg. Chem.* **2007**, 4597–4606. (c) Richardson, C.; Fitchett, C. M.; Keene, F. R.; Steel, P. J. *Dalton Trans.* **2008**, 2534–2537.

(6) (a) Rodionov, V. O.; Fokin, V. V.; Finn, M. G. *Angew. Chem., Int. Ed.* **2005**, *44*, 2210–2215. (b) Huang, S.; Clark, R. J.; Zhu, L. *Org. Lett.* **2007**, *9*, 4999–5002. (c) Donnelly, P. S.; Zanatta, S. D.; Zammit, S. C.; White, J. M.; Williams, S. J. *Chem. Commun.* **2008**, 2459–2461.

(7) (a) Li, Y.; Huffman, J. C.; Flood, A. H. *Chem. Commun.* **2007**, 2692–2694. (b) Meudtner, R. M.; Ostermeier, M.; Goddard, R.; Limberg, C.; Hecht, S. *Chem.—Eur. J.* **2007**, *13*, 9834–9840. (c) Schuster, E. M.; Botoshansky, M.; Gandelman, M. *Angew. Chem., Int. Ed.* **2008**, *47*, 4555–4558. (d) Fletcher, J. T.; Bumgarner, B. J.; Engels, N. D.; Skoglund, D. A. *Organometallics* **2008**, *27*, 5430–5433. (e) Schulze, B.; Friebe, C.; Hager, M. D.; Winter, A.; Hoogenboom, R.; Goerls, H.; Schubert, U. S. *Dalton Trans.* **2009**, 787–794.

(8) Happ, B.; Friebe, C.; Winter, A.; Hager, M. D.; Hoogenboom, R.; Schubert, U. S. *Chem.—Asian J.* **2009**, *4*, 154–163.

(9) Analogue procedure: Bianchini, C.; Giambastiani, G.; Rios, I. G.; Meli, A.; Oberhauser, W.; Sorace, L.; Toti, A. *Organometallics* **2007**, *26*, 5066–5078.

(10) Nakano, Y.; Ishizuka, K.; Muraoka, K.; Ohtani, H.; Takayama, Y.; Sato, F. *Org. Lett.* **2004**, *6*, 2373–2376.

SCHEME 1. Schematic Representation of the Synthesis of the *N*-Heterocyclic Ligands and Their Corresponding Heteroleptic Ruthenium(II) Complexes

Synthesis of the donor and acceptor ligand systems

Synthesis of the ruthenium(II) complexes

$R^1 = O-C_6H_{13}, R^2 = H, R^3 = C_{10}H_{21}$
$R^1 = NO_2, R^2 = H, R^3 = C_{10}H_{21}$
$R^1 = CF_3, R^2 = H, R^3 = C_{10}H_{21}$
$R^1 = H, R^2 = NO_2, R^3 = C_{10}H_{21}$
$R^1 = H, R^2 = H, R^3 = C_{10}H_{21}$
$R^1 = NO_2, R^2 = H, R^3 = Ph$

in quantitative yield. Subsequently, the ligands **10a−d** were obtained in good to high yields (70−93%) utilizing the straightforward Sonogashira cross-coupling with 2−4 mol % of the palladium(0) catalyst. All final products were purified by column chromatography on silica and the purity was confirmed by elemental analysis, high-resolution mass spectrometry (HR-ESI-MS), as well as ^{1}H and ^{13}C NMR spectroscopy.

The second route turned out to be also a versatile way to introduce an aromatic substituent in the N^1-position of the triazole as an alternative to the decyl-moiety in **10** (Scheme 4). Substitution of the flexible alkyl-chain by a more rigid phenyl ring should enhance the growth of single crystals, in particular of the targeted heteroleptic Ru[II] complexes. For this purpose, **6** was allowed to react with phenylazide[8] using the CuAAC reaction

yielding compound **11** (45%) after cleavage of the isopropanol protection group (Scheme 4). Finally, the N^1-phenyl-substituted compound **12** was obtained by Sonogashira cross-coupling reaction in good yield (77%).

Besides the systems featuring donor or acceptor units attached to the pyridine ring (**5**, **10**, and **12**), also derivatives with similar substituents in the N^1-position of the 1*H*-[1,2,3]triazole subunit were in the focus (Scheme 5). For this purpose, (1-azidophenyl)boronic acid[8] and 2-ethynylpyridine were conjugated by using the CuAAC reaction yielding **13**. The purification steps, i.e. simple filtration and recrystallization from ethanol, fully met the criteria of a "click reaction" as defined by Sharpless et al.[3a] Following two times the standard protocol for the Sonogashira cross-coupling reaction, the final

SCHEME 2. **Schematic Representation of the Synthesis of the Donor-Type Ligand 5**
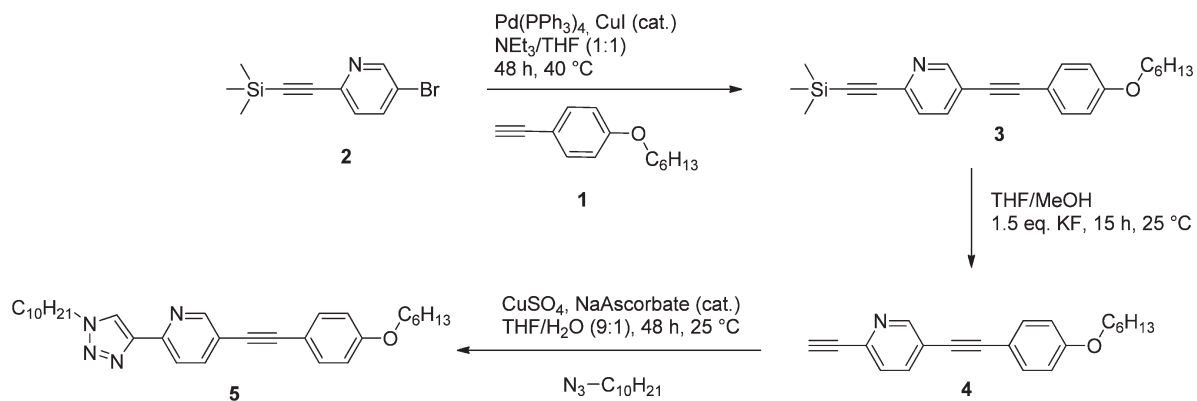
SCHEME 3. **Schematic Representation of the Synthesis of the Acceptor-Type Ligands 10**

10a, R^1 = NO_2, R^2 = H
10b, R^1 = H, R^2 = NO_2
10c, R^1 = CF_3, R^2 = H
10d, R^1 = H, R^2 = H
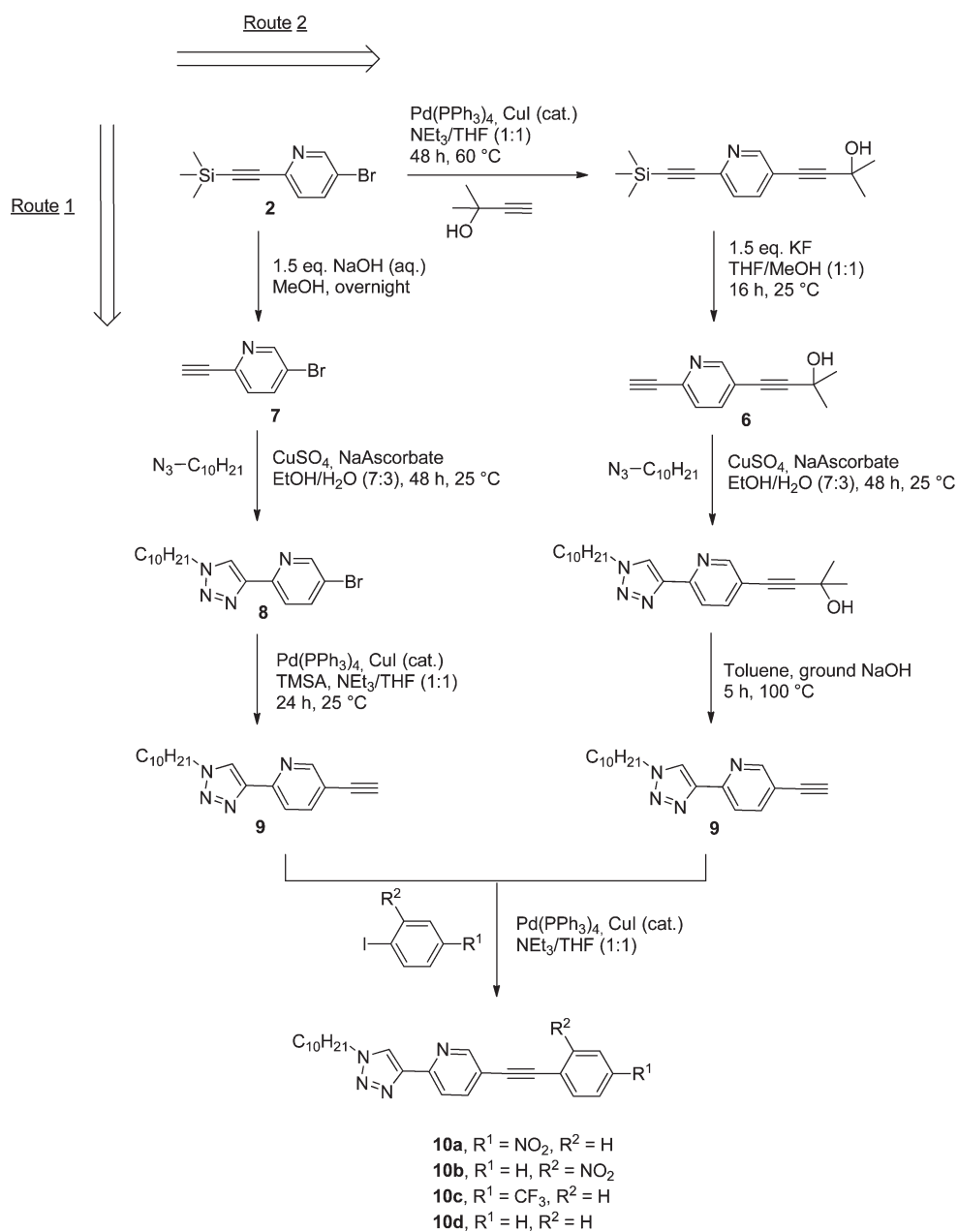
SCHEME 4.   **Schematic Representation of the Synthesis of the Acceptor-Type Ligand 12 Bearing an Aromatic Moiety**
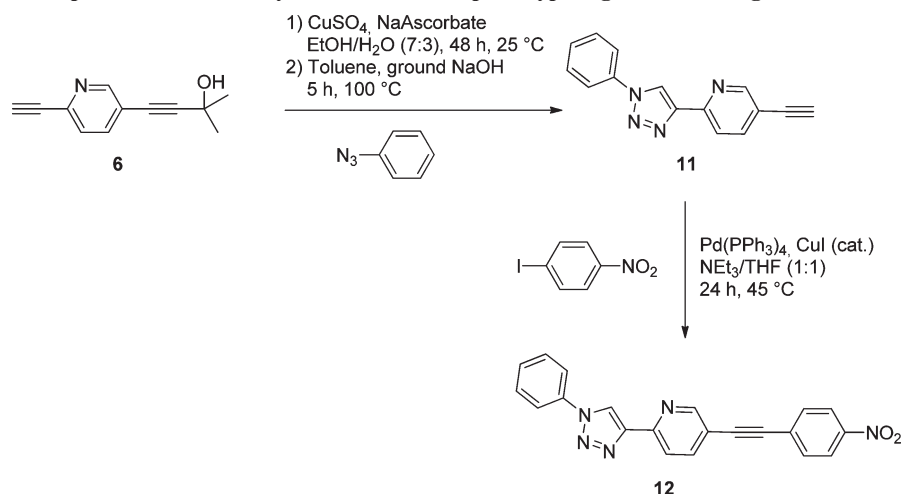
SCHEME 5.   **Schematic Representation of the Synthesis of a 2-(1*H*-[1,2,3]Triazol-4-yl)pyridyl Ligand with an Acceptor-Unit Attached on the Triazole Ring**
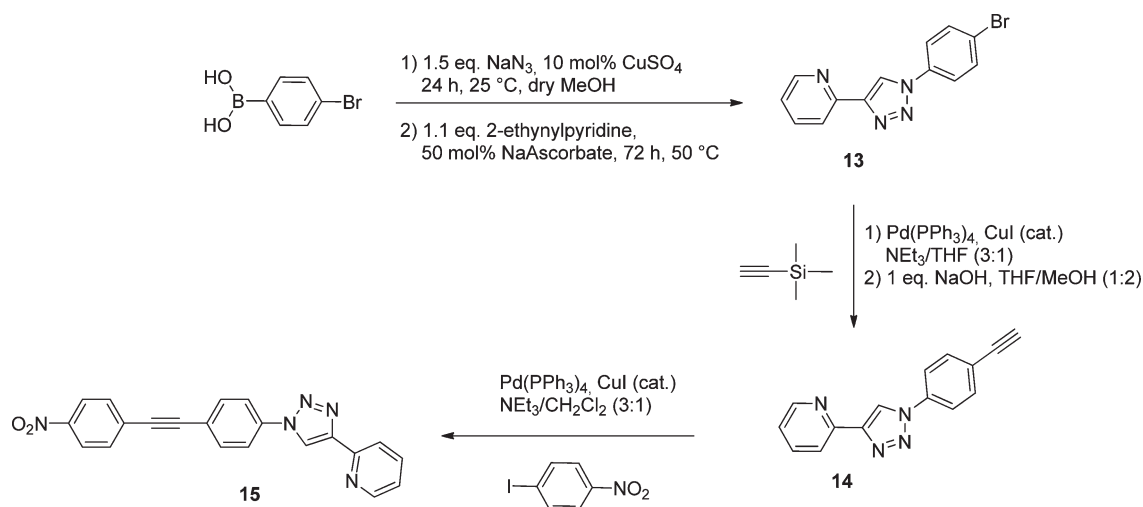
acceptor-functionalized compound **15** was synthesized in moderate yield (50%). However, the implementation of the *O*-alkyl donor system in analogy to **5** was not yet successful.

The heteroleptic ruthenium(II) complexes **16** to **18** of the general structure [(dmbpy)$_2$Ru**L**](PF$_6$)$_2$ (dmbpy = 4,4′-di-methyl-2,2′-bipyridine) were synthesized by heating Ru-(dmbpy)$_2$Cl$_2$[8,11] and the appropriate ligands (**L** = **5**, **10**, **12**, **15**) under microwave irradiation (Table 1). After 2 h the reactions were completed and a 10-fold excess of NH$_4$PF$_6$ was added to precipitate the products. In most cases, precipitation occurred after 15 min and the pure complex was isolated after washing with ethanol and diethyl ether in moderate to very good yields (Table 1). Only **16c** and **17** had to be recrystallized from ethanol/water. The latter fact may explain the moderate yields obtained for these complexes. The verification of the structures of **16**−**18** was carried out by ^{1}H and ^{13}C NMR spectroscopy as well as HR-ESI mass spectrometry.

Crystallographic Analysis. For the heteroleptic Ru^{II} complex **17** single crystals suitable for X-ray crystallographic analysis were obtained by slow diethyl ether diffusion revealing the coordination of the two 4,4′-dimethyl-2,2′-bipyridine and the 2-(1*H*-[1,2,3]triazol-4-yl)pyridine ligand **12** to the Ru^{II} core. The molecule crystallizes in a triclinic system with *P*$\bar{1}$ symmetry (for ORTEP see the Supporting Information). The structural parameters observed from **17** were compared to the corresponding structurally related homoleptic complex [Ru(bpy)$_3$](PF$_6$)$_2$[12] (Figure 2).
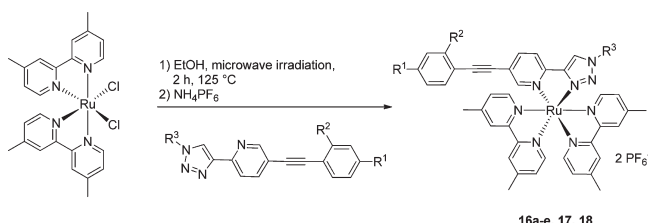
It is noteworthy that the interligand angle of the nitrogen atoms in the square plane were similar for both complexes (**17**: 170.40° and 174.40°; [Ru(bpy)$_3$](PF$_6$)$_2$: 172.3°; see Figure 2) resulting in a comparable distortion of the ideal octahedral geometry. The bond length from ruthenium to the coordinating nitrogen atom of the triazole ring (N′: 2.028(2), Figure 2) was shortened significantly compared

(11) Rau, S.; Ruben, M.; Büttner, T.; Temme, C.; Dautz, S.; Görls, H.; Rudolph, M.; Walther, D.; Vos, J. G. *J. Chem. Soc., Dalton Trans.* **2000**, 3649–3657.
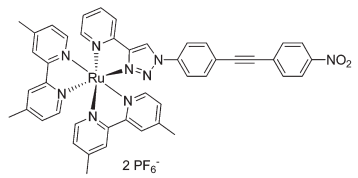
(12) Biner, M.; Buergi, H. B.; Ludi, A.; Roehr, C. *J. Am. Chem. Soc.* **1992**, *114*, 5197–5203.
(13) Egbe, D. A. M.; Bader, C.; Nowotny, J.; Günther, W.; Klemm, E. *Macromolecules* **2003**, *36*, 5459–5469.

TABLE 1. Synthesis of the Heteroleptic Ruthenium(II) Complexes

Entry	Compound	Product	Yield (%)
1	**16a**	$R^1 = OC_6H_{13}$ $R^2 = H$ $R^3 = n\text{-}C_{10}H_{21}$	81
2	**16b**	$R^1 = NO_2$ $R^2 = H$ $R^3 = n\text{-}C_{10}H_{21}$	88
3	**16c**	$R^1 = CF_3$ $R^2 = H$ $R^3 = n\text{-}C_{10}H_{21}$	48
4	**16d**	$R^1 = H$ $R^2 = NO_2$ $R^3 = n\text{-}C_{10}H_{21}$	90
5	**16e**	$R^1 = H$ $R^2 = H$ $R^3 = C_{10}H_{21}$	75
6	**17**	$R^1 = NO_2$ $R^2 = H$ $R^3 = phenyl$	63
7	**18**		77

FIGURE 2. A comparison of bond angles and bond lengths derived from the crystallographic analysis. Left: Ru^{II} complex **17**. Right: Ru(bpy)$_3$(PF$_6$)$_2$.[12]

FIGURE 3. Cyclic voltammograms of ruthenium(II) complexes **16a** to **16e** (10^{-4} M, CH$_3$CN containing 0.1 M TBAPF$_6$).

electrochemical properties are presented in Table 2 and Figure 3.

In all cases a first reversible oxidation wave occurred at around 0.85 V (vs Fc/Fc$^+$) that can be assigned to a Ru^{II}/Ru^{III} oxidation process. Furthermore, compound **16a** showed a second oxidation process at 1.28 V, probably originating from an oxidation process of the triazole ligand. Due to the absence of electron-donating substituents at the triazole ligand, the respective ligand-centered π-orbitals are more stabilized for complexes **16b–e** and, therefore, no such oxidation processes were visible in the CV spectrum.

In contrast to the other systems, the nitro-containing complexes **16b** and **16d** featured a single reversible reduction wave at around -1.35 V vs Fc/Fc$^+$ that could be assigned to a triazole ligand-based reduction process. Both complexes provided a strongly electron-withdrawing substituent causing a stabilization of the triazole-ligand-located antibonding

to that of the adjacent coordinating nitrogen atom of the bipyridine ring (N: 2.052(1), Figure 2). In contrast, the bond length of the opposed coordinating nitrogen to the triazole nitrogen was not reduced but comparable to that of bipyridine. This observation could be rationalized by the expected higher π-acceptor strength of the triazole ring and, consequently, the increased π-back-bonding resulting in a reduced bond length. Additionally, the distance between the ruthenium center and the nitrogen atom of the pyridine moiety of **12** was elongated considerably (N: 2.102(1), Figure 2). This fact derives from a reduction of electron density of this bond in concert with an increased π-back-bonding toward the triazole ring.

Electrochemical Properties. The complexes **16a–e** were subsequently characterized by cyclic voltammetry (CV). The

TABLE 2. Electrochemical Data of Selected Ru^{II} Complexes

complex	$E_{1/2,ox}$ [V]^a	$E_{1/2,red}$ [V]^a	E_g^{opt} [eV]^b	E^{HOMO} [eV]^c	E^{LUMO} [eV]^c
16a	0.82, 1.28	$-1.85, -2.06, -2.23$	2.48	-5.62	-3.18
16b	0.88	$-1.34, -1.97, -2.18$	2.43	-5.67	-3.70
16c	0.84	$-1.89, -2.13$	2.44	-5.69	-3.21
16d	0.88	$-1.36, -1.98, -2.11$	2.43	-5.64	-3.62
16e	0.84	$-1.85, -2.03, -2.18$	2.49	-5.64	-3.17

^{a}Measurements were performed in CH$_3$CN containing 0.1 M TBAPF$_6$. The potentials are given vs ferrocene/ferricinium (Fc/Fc$^+$) couple. ^{b}Estimated from the UV–vis spectra at 10% of the maximum of the longest-wavelength absorption band on the low-energy side. ^{c}Determined using $E^{HOMO} = -[(E_{onset,ox} - E_{onset,Fc/Fc+}) - 4.8]$eV and $E^{LUMO} = -[(E_{onset,red} - E_{onset,Fc/Fc+}) - 4.8]$eV, respectively.[13]
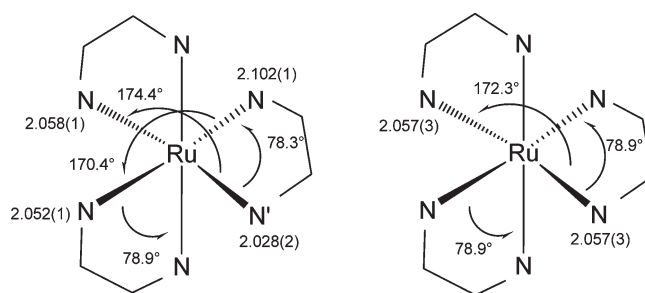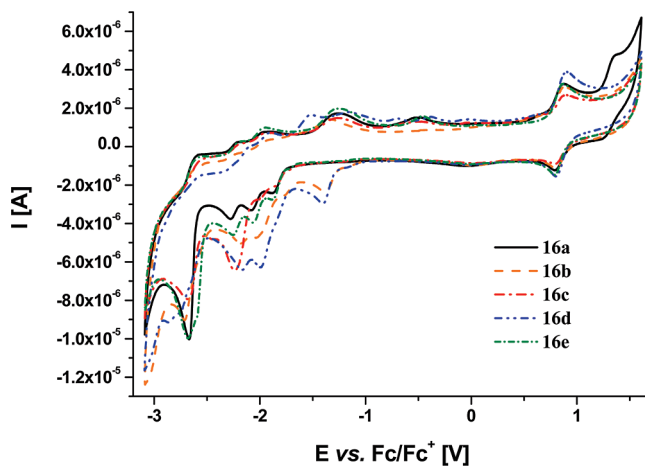
TABLE 3. Photophysical Data of the Donor- and Acceptor-Type Ligands

compound	λ_{abs} [nm] (ε [10^3 L·mol^{-1}·cm^{-1}])^a	λ_{em} [nm]^a
5	250 (2), 323 (32), 338 (30)	378
10a	273 (26), 343 (47)	—^{b}
10b	271 (30), 315 (33), 338 (21)	—^{b}
10c	297 (24), 315 (32), 329 (26)	363
10d	297 (24), 315 (29), 329 (25)	358
12	270 (18), 342 (25)	—^{b}

^{a}For all measurements: 10^{-6} M solution (CH$_2$Cl$_2$). For emission measurements: excitation at longest absorption wavelength. ^{b}No emission detectable at room temperature.

π^*-orbitals (*q.v.* results of the DFT calculations). Starting at -1.8 V all five complexes showed additional reduction waves deriving from ligand-based (dmbpy and triazole ligand) π^*-orbitals.

Photophysical Properties. The UV−vis absorption and emission data of the donor- and acceptor-type systems are depicted in Table 3. As expected, ligand **10a** (nitro-moiety in the para-position) revealed the largest bathochromic shift in the absorption spectrum, but did not show fluorescence at room temperature. In contrast to **10a**, the donor-system **5** as well as the acceptor ligands without nitro groups (**10c/d**) revealed room temperature emission. Compound **5** showed the largest Stokes shift of 3130 cm^{-1} whereas **10c** and **10d** featured remarkably small Stokes shifts (**10c**: 1220 cm^{-1}; **10d**: 1240 cm^{-1}). The reason for the large Stokes shift of **5** was probably caused by the charge transfer nature of the electronic transition.

The optical properties of the heteroleptic ruthenium(II) complexes are summarized in Table 4. A common feature of all complexes was a broad absorption band at around 400 to 500 nm, which could be assigned mainly to various metal-to-ligand charge-transfer (MLCT) transitions between the ruthenium metal center and either the 4,4′-dimethyl-2,2′-bipyridine or the triazole ligand (see DFT calculations). All complexes possessed extinction coefficients of about 20 000 M^{-1}·cm^{-1}, whereas the alkoxy and the unsubstituted systems showed slightly higher values (24 000 and 21 000 M^{-1}·cm^{-1}) than their trifluoromethyl (18 000 M^{-1}·cm^{-1}) or even nitro counterparts (12 000 and 13 000 M^{-1}·cm^{-1}). Between 300 and 400 nm, the complexes investigated herein exhibited different absorption behavior concerning their wavelength maxima and band shape. Therefore, this region seemed to be dominated by intraligand (IL) transitions, namely located at the triazole ligand. A comparison with the respective absorption spectra of triazole ligands (Table 3) supported this assumption. At 286 nm a strong absorption (65 000 to 135 000 M^{-1}·cm^{-1}) could be observed for all complexes, most likely originating from a dmbpy-located IL

transition. More bands were present below 280 nm that arose from further MLCT, ligand-to-ligand charge transfer (LLCT) and metal-centered (MC) d−d transitions, respectively.

The observed emission energies (Table 4) showed a clear dependency on the used substituent. Starting at 602 nm in the case of the alkoxy-containing system, the emission was strongly red-shifted to 621 nm for the unsubstituted triazole ligand and to 640 and even 674 nm in the case of the complexes possessing an *o*- and *p*-nitrophenyl moiety, respectively. This trend was most likely caused by the stabilization of the π^*-orbitals located at the triazole ligand via introduction of electron-withdrawing groups. These orbitals are, at least in case of electron-acceptor substituents, supposed to be involved in the emissive ^{3}MLCT state, so that a lower energy level led to decreased emission energy.

Also depicted in Table 4 are the photoluminescence quantum yields (Φ_{PL}) of the ruthenium(II) systems. At least in aerated acetonitrile, the Φ_{PL} values were rather low (around 0.1% for **16a−e**, nearly no emission in the case of phenyl-substituted **17** and about 0.3% for the "inverse" system **18**). When changing to dichloromethane as solvent, the emission efficiencies rose and a significant difference between the donor- (**16a**) and the acceptor-substituted complex (**16b**) became obvious (0.5% and 2.2%, respectively).

DFT Calculations. To gain a more detailed insight into the photophysical properties of the acceptor- and donor-based complexes, density functional theory (DFT) and time-depended (TD) DFT (B3LYP/6-31G*) calculations were performed. DFT/TD-DFT studies on Ru(II) polypyridyl complexes have been successfully used to understand and rationalize the experimental photophysical features of these complexes.[15] Figure 4 shows the obtained Kohn−Sham frontier orbitals and energy level schemes of the ground state optimized geometries of complexes **16a** and **16b**. In complex **16b** the highest occupied molecular orbitals (HOMOs) were the set t$_{2g}$ of the central Ru^{II} atom. A π-orbital localized in the 2-(1*H*-[1,2,3]triazol-4-yl)-pyridine ligand (π_L) was lower in energy corresponding to the HOMO-3. These orbitals were in different order in the complex **16a**: The π_L corresponded to the HOMO orbital and the set t$_{2g}$ of orbitals was found lower in energy. Both complexes **16a** and **16b** also differed in the order of the lowest unoccupied molecular orbitals (LUMO). In the case of the acceptor-type compound the LUMO orbital corresponded to a π-antibonding orbital located in the 2-(1*H*-[1,2,3]triazol-4-yl)-pyridine ligand (π^*_L), while this orbital was shifted to the LUMO+2 in complex **16a**. In **16a** the LUMO possessed π-antibonding character and was located on the dmbpy ligand (π^*_{dmbpy}). Substitution of the 2-(1*H*-[1,2,3]triazol-4-yl)pyridine ligand with an electron-donating or -withdrawing group,

TABLE 4. Photophysical Data Recorded for the Ru^{II} Complexes

complex	λ_{abs} [nm] (ε [10^3 L·mol^{-1}·cm^{-1}])^{a,b}	λ_{em} [nm]^a	Φ_{PL}^{a,c}
16a	206 (145.6), 286 (133.1), 333 (59.8), 435 (23.6)	602	0.001 [0.005^d]
16b	209 (58.4), 286 (63.4), 328 (38.6), 441 (11.6)	674	0.001 [0.022^d]
16c	209 (88.1), 286 (103.9), 312s (51.6), 440 (18.3)	620	0.002
16d	208 (66.6), 286 (74.7), 341s (22.6), 442 (12.4)	640	0.001
16e	205 (131.1), 286 (125.6), 315s (60.9), 438 (20.6)	621	0.001
17	206 (83.7), 286 (76.9), 326 (52.5), 440 (12.8)	642	< 0.001
18	195 (102.9), 286 (83.1), 316s (40.5), 442s (12.5)	610	0.003

^{a}For all measurements: 10^{-6} M solution in aerated CH$_3$CN at room temperature. For emission measurements: excitation at longest absorption wavelength. ^{b}"s" signifies absorption shoulder. ^{c}Photoluminescence quantum yields determined with [Ru(bpy)$_3$](PF$_6$)$_2$ (Φ_{PL} = 0.062) as standard.[14] ^{d}Measured in aerated CH$_2$Cl$_2$ solution at room temperature (10^{-6} M).
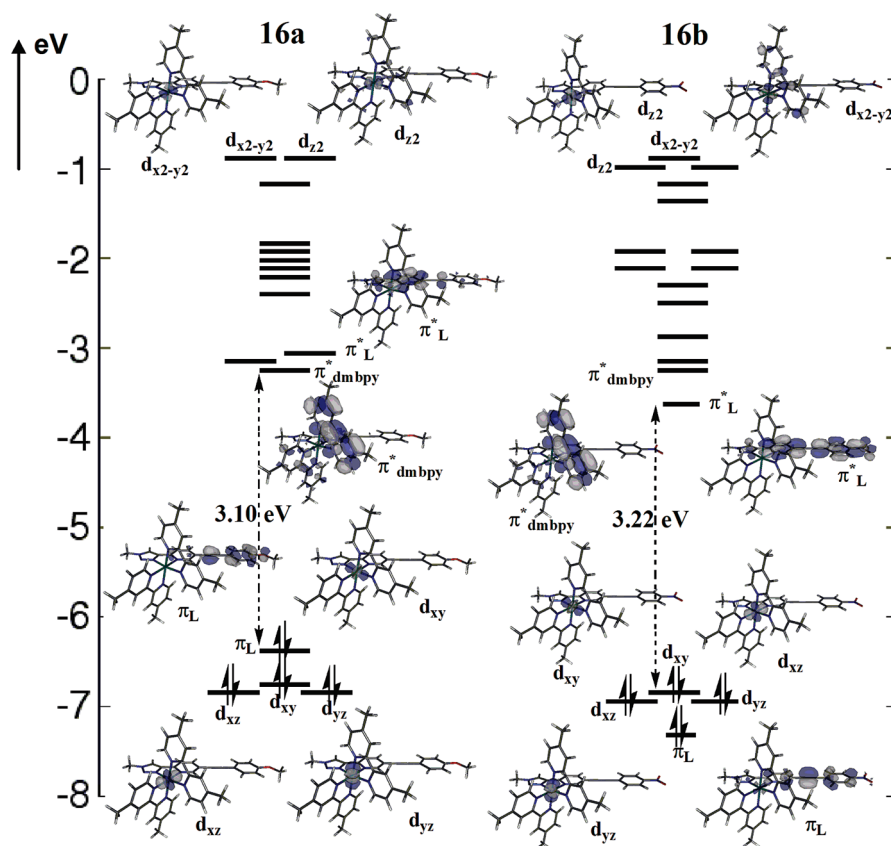
FIGURE 4. Energy level scheme for the Kohn−Sham orbitals of complexes **16a** and **16b**, including the most relevant Kohn−Sham orbitals and the HOMO−LUMO gaps calculated with B3LYP/6-31G*.

respectively, had therefore an important influence on the energy level and ordering of the molecular orbitals.

The set e_g of Ru^{II} orbitals was, as shown in Figure 4, strongly destabilized. Thus, the d_{z^2} and $d_{x^2−y^2}$ orbitals corresponded to LUMO+10 and LUMO+11 in complex **16a**, respectively, while in complex **16b** they related to the orbitals LUMO+12 and LUMO+14. The energetic gaps between the HOMO and LUMO levels are also shown in Figure 4. We obtained theoretical HOMO−LUMO gaps of 3.10 and 3.22 eV for **16a** and **16b**, respectively.

Figure 5 shows the theoretical UV−vis spectra of complexes **16a** and **16b** vs the experimental ones. Table 5 collects the main TD-DFT electronic excitations recorded in the presence of solvent (i.e., CH$_2$Cl$_2$). A fairly good agreement between experiment and theory was observed, notwithstanding that TD-DFT generally tends to underestimate the energy of the charge-transfer states,[16] even if it is well-established that hybrid functionals, such as B3LYP, are less affected by this problem.[17] However, the combination of a

hybrid functional and the consideration of solvent effects on the electronic excitations seemed to be a reasonable approach to reproduce the photophysical properties of the ruthenium(II) complexes (with errors amounting to approximately 0.3 eV). The main features of the experimental spectra were reproduced. Three main bands were obtained for both complexes **16a** and **16b**. As seen in Figure 5, no absorption for both compounds was theoretically predicted beyond 470 nm. Experimentally, absorption was recorded up to 500 nm. The tail between 470 and 520 nm, where singlet−singlet excitations are dark or do not exist, should then be attributed to singlet−triplet excitations (due to non-negligible spin−orbit coupling for the ruthenium atom).

The effect of substitution with an acceptor or a donor unit attached in the 5-position of the pyridine ring had a significant influence on the nature as well as on the position of the UV−vis bands. Thus, in the case of **16a**, the low-energy broad band centered around 440 nm could be assigned to different singlet−singlet electronic excitations of MLCT character (see S_4, S_8, and S_9 in Table 5) as well as LLCT character (see S_3 and S_7 in Table 5). Although a very similar broad band was obtained in the case of compound **16b**, the character of the underlying transitions was different. In complex **16b** this band was mainly composed of MLCT states (see S_4, S_5, S_6, and S_8 in Table 5).

The explanation of the different character of the low-energy bands of **16a** and **16b** could be found by analyzing the orbitals involved in these transitions. For instance, the LLCT states (S_3 and S_7) of compound **16b**, which involved

(14) (a) Demas, J. N.; Crosby, G. A. *J. Phys. Chem.* **1971**, *75*, 991–1024. (b) Juris, A.; Balzani, V.; Barigelletti, F.; Campagna, S.; Belser, B.; von Zelewsky, A. *Coord. Chem. Rev.* **1988**, *84*, 85–277.

(15) (a) Vlcek, A., Jr.; Zalis, S. *Coord. Chem. Rev.* **2007**, *251*, 258–287. (b) Charlot, M.-F.; Aukauloo, A. *J. Phys. Chem. A* **2007**, *111*, 11661–11672. (c) Abbotto, A.; Barolo, C.; Bellotto, L.; De Angelis, F.; Grätzel, M.; Manfredi, N.; Marinzi, C.; Fantacci, S.; Yum, J.-H.; Nazeeruddin, M. K. *Chem. Commun.* **2008**, 5318–5320.

(16) Dreuw, A.; Head-Gordon, M. *Chem. Rev.* **2005**, *105*, 4009–4037.

(17) Dreuw, A.; Weisman, J. L.; Head-Gordon, M. *J. Chem. Phys.* **2003**, *119*, 2943–2946.

TABLE 5. Main Theoretical Electronic Transition Energies (ΔE) with Corresponding Oscillator Strengths (f) and Assignment for Complexes **16a** and **16b**

	16a				16b		
state	ΔE (nm)	f	assignment	state	ΔE (nm)	f	assignment
S_1	477	0.003	$d_{xy} \rightarrow \pi^*_{dmbpy}$ (0.53) MLCT	S_1	479	0.010	$d_{xy} \rightarrow \pi^*_L$ (0.66) MLCT
S_2	462	0.003	$d_{xy} \rightarrow \pi^*_{dmbpy}$ (0.59) MLCT	S_2	466	0.011	$d_{xy} \rightarrow \pi^*_{dmbpy}$ (0.65) MLCT
S_3	453	0.056	$\pi_L \rightarrow \pi^*_{dmbpy}$ (0.53) LLCT	S_4	448	0.023	$d_{xz} \rightarrow \pi^*_L$ (0.66) MLCT
S_4	441	0.162	$d_{xy} \rightarrow \pi^*_L$ (0.51) MLCT	S_5	439	0.065	$d_{yz} \rightarrow \pi^*_L$ (0.54) MLCT
S_7	430	0.180	$\pi_L \rightarrow \pi^*_{dmbpy}$ (0.54) LLCT	S_6	433	0.030	$d_{xz} \rightarrow \pi^*_{dmbpy}$ (0.49) MLCT
S_8	425	0.191	$d_{xy} \rightarrow \pi^*_{dmbpy}$ (-0.35) MLCT $\pi_L \rightarrow \pi^*_L$ (0.35) IL	S_8	414	0.136	$d_{yz} \rightarrow \pi^*_{dmbpy}$ (0.40) MLCT $d_{xz} \rightarrow \pi^*_{dmbpy}$ (0.43) MLCT
S_9	420	0.313	$d_{xz} \rightarrow \pi^*_{dmbpy}$ (0.44) MLCT	S_9	395	0.124	$d_{xz} \rightarrow \pi^*_{dmbpy}$ (0.54) MLCT
S_{10}	407	0.104	$d_{xz} \rightarrow \pi^*_L$ (0.63) MLCT	S_{11}	371	1.262	$\pi_L \rightarrow \pi^*_L$ (0.63) IL
S_{11}	401	0.243	$d_{xz} \rightarrow \pi^*_{dmbpy}$ (0.45) MLCT	S_{13}	348	0.039	$d_{yz} \rightarrow \pi^*_L$ (0.54) MLCT
S_{13}	360	0.192	$\pi_L \rightarrow \pi^*_L$ (0.61) IL	S_{27}	312	0.071	$d_{yz} \rightarrow \pi^*_{dmbpy}$ (-0.29) MLCT $d_{xz} \rightarrow \pi^*_{dmbpy}$ (0.30) MLCT $d_{yz} \rightarrow \pi^*_{dmbpy}$ (0.32) MLCT
S_{30}	307	0.094	$d_{yz} \rightarrow \pi^*_{dmbpy}$ (0.51) MLCT	S_{32}	305	0.116	$d_{yz} \rightarrow \pi^*_{dmbpy}$ (0.44) MLCT $d_{xy} \rightarrow \pi^*_{dmbpy}$ (-0.38) MLCT
S_{32}	306	0.034	$d_{xy} \rightarrow \pi^*_{dmbpy}$ (0.37) MLCT	S_{42}	294	0.066	$d_{yz} \rightarrow \pi^*_L$ (0.47) MLCT
S_{47}	282	0.234	$\pi_L \rightarrow \pi^*_L$ (0.52) IL	S_{49}	276	0.284	$\pi_{dmbpy} \rightarrow \pi^*_{dmbpy}$ (0.41) IL
S_{52}	276	0.177	$\pi_{dmbpy} \rightarrow \pi^*_L$ (0.54) LLCT	S_{50}	274	0.419	$\pi_{dmbpy} \rightarrow \pi^*_{dmbpy}$ (0.33) IL
S_{54}	273	0.286	$\pi_{dmbpy} \rightarrow \pi^*_{dmbpy}$ (0.25) LLCT $d_{xz} \rightarrow d_{x^2-y^2}$ (0.24) MC	S_{51}	273	0.286	$\pi_{dmbpy} \rightarrow \pi^*_{dmbpy}$ (0.23) IL $\pi_{dmbpy} \rightarrow \pi^*_{dmbpy}$ (-0.22) IL
S_{55}	273	0.509	$\pi_{dmbpy} \rightarrow \pi^*_L$ (0.27) LLCT $\pi_{dmbpy} \rightarrow \pi^*_{dmbpy}$ (-0.23) IL $\pi_{dmbpy} \rightarrow \pi^*_{dmbpy}$ (0.23) IL	S_{54}	265	0.146	$\pi_L \rightarrow \pi^*_L$ (0.54) IL
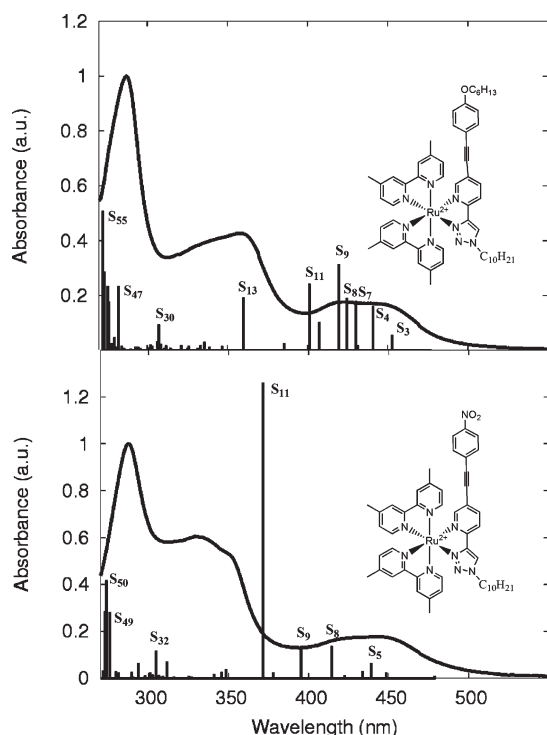
FIGURE 5. Experimental spectra of complexes **16a** (top) and **16b** (bottom) in solid lines superimposed to the TD-DFT (B3LYP/6-31G* in CH_2Cl_2) vertical excitations. The main electronic states are highlighted (see Table 5 for assignments).

electronic transitions from the same π-orbital localized in the 2-(1H-[1,2,3]triazol-4-yl)pyridine ligand (π_L) to different π-antibonding orbitals located on the dmbpy ligands (π^*_{dmbpy}), appeared lower in energy in **16a**. This fact was due to the destabilization of the π_L orbital in the donor-based compound as compared to the same orbital in the acceptor-based compound (recall that the π_L orbital is the HOMO in compound **16a** but the HOMO-3 in **16b**, see Figure 4). The

second band, located experimentally around 360 and 340 nm in complexes **16a** and **16b**, respectively, was characterized by the same electronic excitations (S_{13} and S_{11} for compounds **16a** and **16b**, respectively). These corresponded to intra-ligand (IL) states, which involved local $\pi_L \rightarrow \pi^*_L$ electronic excitations within the 2-(1H-[1,2,3]triazol-4-yl)pyridine ligand. Finally, the most intense peak centered at 286 nm in both complexes was mainly due to IL states in **16b** and states of IL and LLCT character in the case of **16a** (see Table 5). In the case of **16a**, one of these states (S_{54}) was mixed with a MC transition, involving an electronic excitation from the d_{xz} orbital to the unoccupied $d_{x^2-y^2}$ orbital.

Concerning the emission behavior, the trzpy-type ligand systems are known to be potential luminescence quenchers and the ruthenium(II) complexes reported previously did not show any luminescence at room temperature.[7e,8] Also the complexes presented in this contribution showed only very weak emission intensities (see Table 4). For excited Ru[II] polypyridyl complexes it is well-known that the triplet excited states are populated rapidly via efficient intersystem crossings (ISC) from the singlet photoexcited states[18] (due to the strong spin−orbit coupling of the ruthenium center). Afterward, relaxation to the lowest triplet excited state (T_1) follows. Obviously, the nature of the low-lying singlets and triplets excited states should determine the effectiveness of the ISC. As revealed, different singlet excited states were obtained for complexes **16a** and **16b** and, consequently, a different emission behavior was expected. We are currently developing a methodology to estimate the phosphorescence rates and the quantum yields, based on accurate estimation of the spin−orbit couplings between the singlet and triplet manifolds which, in turn, determine the ISC rates.

Conclusions

New 2-(1H-[1,2,3]triazol-4-yl)pyridine bidentate ligands were synthesized as bipyridine analogs, whereas different

(18) Bhasikuttan, A. C.; Suzuki, M.; Nakashima, S.; Okada, T. *J. Am. Chem. Soc.* **2002**, *124*, 8398–8345.

phenylacetylene moieties of donor and acceptor nature, respectively, were attached at the 5-position of the pyridine unit. The moieties featured a crucial influence on the electronic properties of these ligands. In addition, the *N*-heterocyclic ligands were coordinated to the ruthenium(II) metal ion by using the bis(4,4′-dimethyl-2,2′-bipyridine-)ruthenium(II) precursor. The Ru[II] complex with electron-donor nature revealed considerable weaker luminescence intensity at room temperature in contrast to the one with acceptor capability revealing remarkable luminescence at room temperature in CH$_2$Cl$_2$. Furthermore, 2-(1*H*-[1,2,3]triazol-4-yl)pyridine systems are known to be potential luminescence quenchers at room temperature as soon as they are attached to a ruthenium(II) metal ion. All herein described heteroleptic ruthenium(II) complexes overcame this luminescence quenching and led to room temperature emission in acetonitrile. The highest quantum yield could be found for the Ru[II] complex **16b** (Φ = 0.02) bearing a nitro group in the para-position of the phenylacetylene subunit.

Experimental Section

Materials and Instrumentation. Unless noted otherwise, all reagents were acquired from commercial sources and used without further purification. Solvents were dried and distilled according to standard procedures and stored under argon. If not specified otherwise solvents were degassed by bubbling with argon 1 h before use. All reactions were performed in air-dried flasks under an argon atmosphere unless stated otherwise. Purification of reaction products was carried out by column chromatography with 40−63 μm silica gel. Analytical thin layer chromatography (TLC) was performed on silica sheets precoated with silica gel 60 F254 and visualization was accomplished with UV light (254 nm). The heteroleptic ruthenium(II) complexes were synthesized by microwave-assisted reactions, using a Biotage Initiator ExpEU (maximum power: 400 W; working frequency: 2450 MHz) with closed reaction vials. During the experiments the temperature and the pressure profiles were detected. 1D-(^{1}H and ^{13}C) and 2D-(^{1}H−^{1}H gCOSY) nuclear magnetic resonance spectra were recorded at 298 K. Chemical shifts are reported in parts per million (ppm, δ scale) relative to the signal of the applied solvent. Coupling constants are given in hertz. Data are reported as follows: multiplicity (ap = apparent, br = broad, s = singlet, d = doublet, t = triplet, q = quartet, m = multiplet).

Computational Details. The geometries of **16a** and **16b** were optimized in the electronic singlet ground state using density functional theory (DFT) with the hybrid functional B3LYP[19,20] and the 6-31G* basis set for all atoms. Relativistic effects were included in the Ru atom, using the ECP-28-mwb Stuttgart/Dresden pseudopotential.[21] For computational ease the structures were reduced by substitution of the decyl chain attached to the triazole ring by a methyl group and in the case of compound **16b**, additionally the hexyloxy group of **16a** was replaced by a methoxy group. The lowest-lying 55 vertical singlet electronic excitation energies were obtained by using TD-DFT at the S$_0$ optimized geometries. This calculation was performed in solution with CH$_2$Cl$_2$ as solvent with the polarization continuum model,[22,23] (ε = 8.93). All the calculations were performed with the Gaussian03 program package.[24]

1-Ethynyl-4-(hexyloxy)benzene (1).[25] 1-Iodo-4-(hexyloxy)-benzene (1.5 g, 4.93 mmol), tetrakis(triphenylphosphine)-palladium(0) (114 mg, 0.1 mmol), and CuI (20 mg, 0.1 mmol) were dissolved in a degassed NEt$_3$/THF mixture (3:7 ratio, 35 mL) at room temperature. After trimethylsilylacetylene (0.7 mL, 4.93 mmol) was added quickly through a syringe, the solution was stirred for 24 h at room temperature. The salts formed were filtered off, and the solution was evaporated under reduced pressure. The yellow oil was purified by a chromatographic filtration over a silica gel pad (toluene as eluent) yielding pure 1-(trimethylsilyl)ethynyl-4-(hexyloxy)benzene. Subsequently, the silylated compound was dissolved in a mixture of THF and methanol and aq NaOH (5 M, 1 mL) was added. The reaction mixture was stirred overnight at room temperature and then extracted with dichloromethane after adding brine (50 mL). The organic extract was dried over anhydrous MgSO$_4$ and subsequent gel filtration (silica, toluene) afforded the pure, colorless product (0.91 g, 91%).

5-Bromo-2-((trimethylsilyl)ethynyl)pyridine (2).[26] 2,5-Dibromopyridine (3.5 g, 14.8 mmol), tetrakis(triphenylphosphine)-palladium(0) (347 mg, 0.3 mmol), and CuI (57 mg, 0.3 mmol) were dissolved in a degassed NEt$_3$/THF mixture (3:7 ratio, 50 mL) at 0 °C. After trimethylsilylacetylene (2.09 mL, 14.8 mmol) was added quickly through a syringe, the solution was stirred for 2 h at 0 °C and was then allowed to stir at room temperature overnight. The salts formed were filtered off, and the solution was evaporated under reduced pressure. The dark orange oil was purified by a chromatographic filtration over a silica gel pad (toluene as eluent) providing the product as yellow oil, which solidifies upon standing at room temperature after one week. Finally, purification by gentle sublimation (3.3 × 10^{-2} mbar, 60 °C) afforded the pure product as a white powder (3.25 g, 86%).

2-Ethynyl-5-((4-(hexyloxy)phenyl)ethynyl)pyridine (4). 5-Bromo-2-((trimethylsilyl)ethynyl)pyridine (**2**, 1.0 g, 4 mmol), 1-ethynyl-4-(hexyloxy)benzene (**1**, 0.8 g, 4 mmol), tetrakis(triphenylphosphine)palladium(0) (90 mg, 0.08 mmol), and CuI (16 mg, 0.08 mmol) were dissolved in a degassed NEt$_3$/THF mixture (3:7 ratio, 35 mL) at room temperature and the solution was stirred for 48 h at room temperature. The salts formed were filtered off, and the solution was evaporated under reduced pressure. The dark red oil was purified by a gel filtration over silica (toluene as eluent). The obtained 2-(trimethylsilyl)-ethynyl-5-((4-(hexyloxy)phenyl)ethynyl)pyridine was desilylated by dissolving in THF/MeOH (1:2 ratio, 30 mL) and treating with an equimolar amount of potassium fluoride. The red solution was stirred overnight under an argon atmosphere. After that the reaction mixture was concentrated under vacuum and

(19) Becke, A. D. *J. Chem. Phys.* **1993**, *98*, 5648–5652.

(20) Lee, C. T.; Yang, W. T.; Parr, R. G. *Phys. Rev. B* **1988**, *37*, 785–789.

(21) Andrae, D.; Häusermann, U.; Dolg, M.; Stoll, H.; Preuss, H. *Theor. Chim. Acta* **1990**, *77*, 123–141.

(22) Cossi, M.; Barone, V.; Menucci, B.; Tomasi, J. *Chem. Phys. Lett.* **1998**, *286*, 253–260.

(23) Menucci, B.; Tomasi, J. *J. Chem. Phys.* **1997**, *106*, 5151–5158.

(24) Frisch, M. J.; Trucks, G. W.; Schlegel, H. B.; Scuseria, G. E.; Robb, M. A.; Cheeseman, J. R.; Montgomery, J. A., Jr.; Vreven, T.; Kudin, K. N.; Burant, J. C.; Millam, J. M.; Iyengar, S. S.; Tomasi, J.; Barone, V.; Mennucci, B.; Cossi, M.; Scalmani, G.; Rega, N.; Petersson, G. A.; Nakatsuji, H.; Hada, M.; Ehara, M.; Toyota, K.; Fukuda, R.; Hasegawa, J.; Ishida, M.; Nakajima, T.; Honda, Y.; Kitao, O.; Nakai, H.; Klene, M.; Li, X.; Knox, J. E.; Hratchian, H. P.; Cross, J. B.; Bakken, V.; Adamo, C.; Jaramillo, J.; Gomperts, R.; Stratmann, R. E.; Yazyev, O.; Austin, A. J.; Cammi, R.; Pomelli, C.; Ochterski, J. W.; Ayala, P. Y.; Morokuma, K.; Voth, G. A.; Salvador, P.; Dannenberg, J. J.; Zakrzewski, V. G.; Dapprich, S.; Daniels, A. D.; Strain, M. C.; Farkas, O.; Malick, D. K.; Rabuck, A. D.; Raghavachari, K.; Foresman, J. B.; Ortiz, J. V.; Cui, Q.; Baboul, A. G.; Clifford, S.; Cioslowski, J.; Stefanov, B. B.; Liu, G.; Liashenko, A.; Piskorz, P.; Komaromi, I.; Martin, R. L.; Fox, D. J.; Keith, T.; Al-Laham, M. A.; Peng, C. Y.; Nanayakkara, A.; Challacombe, M.; Gill, P. M. W.; Johnson, B.; Chen, W.; Wong, M. W.; Gonzalez, C.; Pople, J. A. *Gaussian-03*, Revision C.02; Gaussian, Inc., Wallingford, CT, 2004.

(25) Chang, J. Y.; Yeon, J. R.; Shru, Y. S.; Han, M. J.; Hong, S.-K. *Chem. Mater.* **2000**, *12*, 1076–1082.

(26) Bianchini, C.; Giambastiani, G.; Rios, I. G.; Meli, A.; Oberhauser, W.; Sorace, L.; Toti, A. *Organometallics* **2007**, *26*, 5066–5078.

purified by means of gel filtration on silica gel yielding the desired product as a slight yellow powder (1.06 g, 87%). ^{1}H NMR (CDCl$_3$, 300 MHz) δ 8.62 (d, J = 1.3 Hz, 1H), 7.73 (dd, J = 8.1 Hz, J = 2.1 Hz, 1H), 7.49−7.42 (m, 3H), 6.91−6.85 (m, 2H), 3.97 (t, ^3J = 6.6 Hz, 2H), 3.25 (s, 1H), 1.79−1.74 (m, 2H), 1.49−1.30 (m, 6H), 0.91 (t, J = 6.8 Hz, 3H). ^{13}C NMR (CDCl$_3$, 75 MHz) δ 159.8, 152.2, 140.3, 138.1, 133.2, 126.71, 120.7, 114.7, 114.0, 94.9, 84.5, 82.6, 78.6, 68.1, 31.5, 29.1, 25.7, 22.6, 14.0. Anal. Calcd for C$_{21}$H$_{21}$NO: C 83.13, H 6.98, N 4.62. Found: C 82.78, H 7.08, N 4.92.

2-(1-Decyl-1*H*-[1,2,3]triazol-4-yl)-5-((4-(hexyloxy)phenyl)-ethynyl)pyridine (5). A sealed microwave vial with 1-bromodecane (91 mg, 0.41 mmol) and 1.5 equiv of sodium azide (40 mg) in DMSO (5 mL) was heated under microwave irradiation for 1 h at 100 °C. Water was then added to quench the reaction and the product was extracted into diethyl ether, washed with brine, and dried over Na$_2$SO$_4$. The solution was subsequently reduced in vacuo to yield 1-azidodecane (95%). The organic azide, 2-ethynyl-5-((4-(hexyloxy)phenyl)ethynyl)pyridine (**4**, 127 mg, 0.42 mmol), CuSO$_4$ (7 mg, 0.042 mmol, dissolved in 0.5 mL water), and sodium ascorbate (42 mg, 0.21 mmol, dissolved in 1 mL water) were dissolved in THF (15 mL) and the reaction mixture was stirred for 24 h at room temperature. Subsequently, ethylenediaminetetraacetic acid-containing water (60 mL) was added to the reaction mixture and the product was extracted with CH$_2$Cl$_2$. Gel filtration on silica (CHCl$_3$/EtOAc 1:1 ratio) and subsequent column chromatography (silica, CHCl$_3$/EtOAc 20:1 ratio) provided the pure product as white powder (134 mg, 67%). ^{1}H NMR (CDCl$_3$, 300 MHz) δ 8.68 (s, 1H), 8.13−8.11 (m, 2H), 7.86 (dd, J = 8.2 Hz, J = 2.1 Hz, 1H), 7.46−7.42 (m, 2H), 6.86−6.82 (m, 2H), 4.4 (t, J = 7.2 Hz, 2H), 3.97 (t, J = 6.5 Hz, 2H), 1.94−1.88 (m, 2H), 1.79−1.76 (m, 2H), 1.48−1.22 (m, 20H), 0.87−0.81 (m, 6H). ^{13}C NMR (CDCl$_3$, 75 MHz) δ 159.5, 151.6, 148.7, 147.8, 139.0, 133.0, 122.0, 119.6, 119.3, 114.5, 114.3, 93.1, 84.8, 68.0, 50.4, 31.7, 31.5, 30.1, 29.3, 29.2, 29.1, 29.0, 28.9, 26.3, 25.6, 22.5, 22.5, 14.0, 13.9. Anal. Calcd for C$_{31}$H$_{42}$N$_4$O: C 76.50, H 8.70, N 11.51. Found: C 76.52, H 8.79, N 11.71.

4-(6-Ethynylpyridin-3-yl)-2-methylbut-3-yn-2-ol (6).[27] To a degassed solution of 5-bromo-2-[(trimethylsilyl)ethynyl]pyridine (**2**, 1.5 g, 5.9 mmol), CuI (23 mg, 0.12 mmol), and Pd(PPh$_3$)$_4$ (140 mg, 0.12 mmol) in triethylamine (50 mL) was added 2-methyl-3-butyn-2-ol (0.58 mL, 5.9 mmol) and the reaction mixture was stirred for 24 h at 55 °C. The mixture was diluted with diethyl ether, washed once with brine, and dried over MgSO$_4$. Concentration in vacuo yielded the crude product, which was purified by chromatography on silica gel (chloroform/ethyl acetate 4:1) to afford 5-(3-hydroxy-3-methyl-1-butynyl)-2-[(triisopropylsilyl)-ethynyl]pyridine. To a stirred solution of the latter product in methanol (50 mL) was added solid potassium fluoride (1.5 equiv), and the mixture was stirred at room temperature overnight under an argon atmosphere. Subsequently, the reaction mixture was filtered by means of gel filtration on silica gel (chloroform/ethyl acetate 4:1) and concentrated in vacuo yielding the desired product as an orange powder (670 mg, 61%).

5-Bromo-2-ethynylpyridine (7).[28] To a solution of 2,5-dibromopyridine (7 g, 30 mmol), CuI (70 mg, 0.37 mmol), and Pd-(PPh$_3$)$_4$ (260 mg, 0.37 mmol) in degassed NEt$_3$/THF (1:1 ratio, 100 mL) was added trimethylsilylacetylene (4.2 mL, 30 mmol). The mixture was stirred at room temperature overnight under argon atmosphere. After removal of the solvent under reduced pressure, the residue was purified by gel filtration (CHCl$_3$) to yield 2-(trimethylsilyl)ethynyl-5-bromopyridine as off-white powder (6.95 g, 92%). Subsequently, the compound was dissolved in

(27) Nakano, Y.; Ishizuka, K.; Muraoka, K.; Ohtani, H.; Takayama, Y.; Sato, F. *Org. Lett.* **2004**, *6*, 2373–2376.
(28) Tilley, J. W.; Zawoiski, S. *J. Org. Chem.* **1988**, *53*, 386–390.

methanol (80 mL) and treated with aq NaOH (5 M, 12 mL). The yellow solution was stirred overnight, whereupon the solution turned black. Subsequent gel filtration on silica (CHCl$_3$) yielded the product as white powder (3.79 g, 69%).

5-Bromo-2-(1-decyl-1*H*-[1,2,3]triazol-4-yl)pyridine (8). 5-Bromo-2-ethynylpyridine (**7**, 1.04 g, 5.45 mmol) and 1-azidodecane (see synthesis of **5**, 1.0 g, 5.45 mmol) were dissolved in an ethanol/water mixture (7:1 ratio, 70 mL), using a round-bottomed flask (100 mL). Then copper(II) sulfate (80 mg, 0.5 mmol, dissolved in 3 mL of water) and sodium ascorbate (490 mg, 2.5 mmol, dissolved in 4 mL of water) were added. The reaction mixture turned yellow after a while and was stirred for 72 h at 25 °C. The yellow precipitate was filtered and washed with ethanol. After recrystallization from ethanol the pure product was obtained as colorless crystals (1.35 g, 67%). ^{1}H NMR (CDCl$_3$, 300 MHz) δ 8.61 (s, 1H), 8.09−8.07 (m, 2H), 7.89−7.86 (m, 1H), 4.40 (t, J = 7.2 Hz, 2H), 1.94−1.89 (m, 2H), 1.34−1.24 (m, 14H), 0.87−0.81 (m, 3H). ^{13}C NMR (CDCl$_3$, 75 MHz) δ 150.3, 148.9, 147.4, 139.4, 121.9, 121.3, 119.3, 50.5, 31.8, 30.2, 29.4, 29.3, 29.2, 28.9, 26.4, 22.6, 14.0. Anal. Calcd for C$_{17}$H$_{25}$BrN$_4$: C 55.89, H 6.90, N 15.34. Found: C 56.22, H 7.23, N 14.98.

2-(1-Decyl-1*H*-[1,2,3]triazol-4-yl)-5-ethynylpyridine (9, Route 1). 4-(6-Ethynylpyridin-3-yl)-2-methylbut-3-yn-2-ol (**6**, 300 mg, 1.58 mmol) and 1-azidodecane (see synthesis of **5**, 275 mg, 1.5 mmol) were dissolved in an ethanol/water mixture (7:3 ratio, 30 mL), using a round-bottomed flask (100 mL). Then copper(II) sulfate (24 mg, 0.15 mmol, dissolved in 1 mL of water) and sodium ascorbate (150 mg, 0.75 mmol, dissolved in 1 mL of water) were added. The reaction mixture turned green after a while and was stirred for 72 h at 50 °C. Subsequently, an excess of water was poured into the reaction mixture (100 mL) and the crude product precipitated and was filtered off. Gel filtration on silica (CHCl$_3$/EtOAc 1:1) provided 4-(6-(1-decyl-1*H*-[1,2,3]triazole-4-yl)pyridin-3-yl)-2-methylbut-3-yn-2-ol as white powder (490 mg, 85%). This intermediate was dissolved in dry toluene (30 mL). After adding ground NaOH (200 mg, 5 mmol) and KOH (150 mg, 2.6 mmol) the reaction mixture was refluxed for 5 h. Subsequent column chromatography on silica (CHCl$_3$/EtOAc 2:1 ratio) yielded 2-(1-decyl-1*H*-[1,2,3]-triazole-4-yl)-5-ethynylpyridine as transparent crystals (303 mg, 74%). ^{1}H NMR (CDCl$_3$, 300 MHz) δ 8.67 (d, J = 1.6 Hz, 1H), 8.20−8.14 (m, 2H), 7.89−7.83 (m, 1H), 4.41 (t, J = 7.2 Hz, 2H), 3.25 (s, 1H), 1.95−1.89 (m, 2H), 1.34−1.25 (m, 14H), 0.87 (t, J = 6.5 Hz, 3H). ^{13}C NMR (CDCl$_3$, 75 MHz) δ 152.4, 149.7, 147.7, 139.9, 122.2, 119.3, 118.0, 80.8, 80.5, 50.5, 31.8, 30.2, 29.4, 29.3, 29.2, 28.9, 26.4, 22.6, 14.0. Anal. Calcd for C$_{19}$H$_{26}$N$_4$: C 73.51, H 8.44, N 18.05. Found: C 73.50, H 8.24, N 18.38.

2-(1-Decyl-1*H*-[1,2,3]triazol-4-yl)-5-ethynylpyridine (9, Route 2). To a solution of 5-bromo-2-(1-decyl-1*H*-[1,2,3]triazol-4-yl)-pyridine (**8**, 1.0 g, 2.74 mmol), CuI (13 mg, 0.07 mmol), and Pd(PPh$_3$)$_4$ (80 mg, 0.07 mmol) in degassed NEt$_3$/CH$_2$Cl$_2$ (3:1 ratio, 500 mL) was added trimethylsilylacetylene (280 mg, 2.8 mmol). The mixture was stirred 48 h at room temperature under argon atmosphere. After removal of the solvent under reduced pressure, the residue was purified by gel filtration on silica (chloroform). Afterward, the trimethylsilyl-protected product was dissolved in methanol (40 mL) and treated with aq NaOH (5 M, 1 mL). After 5 h the solvent was removed and the crude product was finally purified by gradient column chromatography on silica (CHCl$_3$, CHCl$_3$/EtOAc 3:1 ratio) yielding the product as white powder (470 mg, 55%).

General Procedure of the Sonogashira Reaction. 2-(1-Decyl-1*H*-[1,2,3]triazol-4-yl)-5-ethynylpyridine (0.32 mmol), nitro-substituted 1-iodobenzene (0.32 mmol), tetrakis(triphenylphosphine)palladium(0) (16 mg, 0.012 mmol), and CuI (8 mg, 0.012 mmol) were dissolved in a degassed NEt$_3$/THF mixture (1:1, 10 mL). The solution was stirred for 48 h at 40 °C under argon atmosphere. The salts formed were filtered off, and the solution

was evaporated under reduced pressure. The pure product was isolated by column chromatography over silica.

2-(1-Decyl-1*H*-[1,2,3]triazol-4-yl)-5-((4-nitrophenyl)ethynyl)-pyridine (10a). According to the general procedure the product was synthesized and purified by column chromatography over silica (CHCl$_3$, R_f 0.6) yielding **10a** as a slight yellow powder (128 mg, 93%). ^{1}H NMR (CDCl$_3$, 300 MHz) δ 8.76 (s, 1H), 8.26–8.16 (m, 4H), 7.94–7.90 (m, 1H), 7.71–7.68 (m, 2H), 4.4 (t, J = 7.2 Hz, 2H), 1.99–1.91 (m, 2H), 1.35–1.25 (m, 14H), 0.87–0.81 (m, 3H). ^{13}C NMR (CDCl$_3$, 75 MHz) δ 152.1, 150.0, 147.6, 147.3, 139.5, 132.4, 129.5, 123.7, 122.4, 119.6, 118.1, 91.3, 90.9, 50.6, 31.8, 30.2, 29.4, 29.3, 29.2, 29.0, 26.5, 22.6, 14.1. ESI-TOF MS: m/z 432.24 ([M + H]$^+$). Anal. Calcd for C$_{25}$H$_{29}$N$_5$O$_2$: C 69.58, H 6.77, N 16.23. Found: C 69.21, H 6.72, N 16.58.

2-(1-Decyl-1*H*-[1,2,3]triazol-4-yl)-5-((2-nitrophenyl)ethynyl)-pyridine (10b). According to the general procedure the product was synthesized and purified by column chromatography over silica (CHCl$_3$/EtOAc, 5:1 ratio) yielding **10b** as off-white powder (63 mg, 69%). ^{1}H NMR (CDCl$_3$, 300 MHz) δ 8.76 (s, 1H), 8.21–8.10 (m, 3H), 7.97–7.91 (m, 1H), 7.73–7.69 (m, 1H), 7.63–7.60 (m, 1H), 7.53–7.49 (m, 1H), 4.42 (t, J = 7.2 Hz, 2H), 1.99–1.91 (m, 2H), 1.34–1.24 (m, 14H), 0.88 (t, J = 6.7 Hz, 3H). ^{13}C NMR (CDCl$_3$, 75 MHz) δ 152.2, 150.0, 149.5, 147.7, 139.7, 134.6, 132.9, 129.0, 124.8, 122.4, 119.5, 118.1, 93.8, 88.2, 50.6, 31.8, 30.2, 29.4, 29.3, 29.2, 29.0, 26.4, 22.6, 14.1. ESI-HRMS calcd for C$_{25}$H$_{30}$N$_5$O$_2$ ([M + H]$^+$) 432.2394, found 432.2390.

2-(1-Decyl-1*H*-[1,2,3]triazol-4-yl)-5-((4-(trifluoromethyl)phenyl)ethynyl)pyridine (10c). According to the general procedure, the product was synthesized and purified by column chromatography over silica (CHCl$_3$, R_f 0.5) yielding **10d** as white powder (81 mg, 94%). ^{1}H NMR (CDCl$_3$, 300 MHz) δ 8.72 (s, 1H), 8.21–8.17 (m, 2H), 7.92–7.88 (m, 1H), 7.68–7.61 (m, 4H), 4.42 (t, J = 7.2 Hz, 2H), 1.96–1.90 (m, 2H), 1.34–1.24 (m, 14H), 0.88 (t, J = 6.7 Hz, 3H). ^{13}C NMR (CDCl$_3$, 75 MHz) δ 152.0, 139.5, 131.9, 126.4, 125.6, 125.5, 125.4, 125.4, 125.3, 122.4, 119.5, 118.5, 91.4, 88.5, 50.6, 31.8, 30.2, 29.5, 29.4, 29.2, 29.0, 26.5, 22.7, 14.1. ESI-HRMS calcd for C$_{26}$H$_{30}$F$_3$N$_4$ ([M + H]$^+$) 455.2417, found 455.2408.

5-((4-Phenyl)ethynyl)-2-(1-phenyl-1*H*-[1,2,3]triazol-4-yl)pyridine (10d). According to the general procedure the product was synthesized and purified by column chromatography over silica (CHCl$_3$/EtOAc, 5:1 ratio) yielding **10d** as off-white powder (44 mg, 61%). ^{1}H NMR (CDCl$_3$, 300 MHz) δ 8.74 (s, 1H), 8.16–8.11 (m, 2H), 7.90–7.84 (m, 1H), 7.58–7.54 (m, 2H), 7.39–7.35 (m, 3H), 4.42 (t, J = 7.2 Hz, 2H), 1.96–1.89 (m, 2H), 1.34–1.24 (m, 14H), 0.88 (t, J = 6.7 Hz, 3H). ^{13}C NMR (CDCl$_3$, 75 MHz) δ 151.8, 139.3, 131.7, 128.8, 128.4, 122.6, 122.2, 119.5, 119.4, 93.1, 86.1, 50.6, 31.8, 30.2, 29.4, 29.3, 29.2, 29.0, 26.4, 22.6, 14.1. ESI-HRMS calcd for C$_{25}$H$_{30}$N$_4$Na ([M + Na]$^+$) 409.2363, found 409.2334.

5-Ethynyl-2-(1-phenyl-1*H*-[1,2,3]triazol-4-yl)pyridine (11). Sodium azide (330 mg, 5.1 mmol) and anhydrous CuSO$_4$ (54 mg, 0.34 mmol) were dissolved in abs methanol (30 mL). Phenylboronic acid (414 mg, 3.4 mmol) was added to the brown solution and the reaction mixture was stirred for 48 h at room temperature. The conversion was controlled by TLC on silica (CHCl$_3$). The slightly green solution was concentrated to 10 mL in vacuum and, subsequently, THF (20 mL), sodium ascorbate (336 mg, 1.7 mmol, in 1 mL of water), 4-(6-ethynylpyridin-3-yl)-2-methylbut-3-yn-2-ol (600 mg, 3.24 mmol), and water (4 mL) were added. The reaction was stirred for 72 h at 50 °C. After that, an excess of water was added to the reaction mixture and the precipitate was filtered off. The filtrate was cautiously extracted with CHCl$_3$ and the organic extract was combined with the precipitate. The CHCl$_3$ solution was dried over NaSO$_4$ and filtered. Column chromatography on silica (CHCl$_3$/EtOAc, 2:1 ratio) provided the (2-methylbut-3-yn-2-ol)-protected product as a white powder. The deprotection was accomplished by refluxing overnight in toluene with ground NaOH

(1.5 equiv). The toluene solution was washed with water and subsequent gel filtration on silica provided the pure desired product (360 mg, 45%). ^{1}H NMR (CDCl$_3$, 300 MHz) δ 8.71 (s, 1H), 8.61 (s, 1H), 8.23 (d, J = 8.2 Hz, 1H), 7.90 (dd, J = 8.2 Hz, J = 2.0 Hz, 1H), 7.83–7.80 (m, 2H), 7.59–7.44 (m, 3H), 3.28 (s, 1H, CH). ^{13}C NMR (CDCl$_3$, 75 MHz) δ 152.5, 149.2, 148.3, 140.0, 136.8, 129.9, 128.9, 120.4, 119.6, 118.3, 81.0, 80.5. Anal. Calcd for C$_{15}$H$_{10}$N$_4$: C 73.16, H 4.09, N 22.75. Found: C 73.49, H 3.78, N 22.50.

5-((4-Nitrophenyl)ethynyl)-2-(1-phenyl-1*H*-[1,2,3]triazol-4-yl)pyridine (12). 5-Ethynyl-2-(1-phenyl-1*H*-[1,2,3]triazol-4-yl)pyridine (**11**, 75 mg, 0.3 mmol), 1-iodo-4-nitrobenzene (76 mg, 0.3 mmol), tetrakis(triphenylphosphine)palladium(0) (8 mg, 0.006 mmol), and CuI (2 mg, 0.006 mmol) were dissolved in a degassed NEt$_3$/THF mixture (3:1 ratio, 10 mL) and the solution was stirred for 48 h at 40 °C under argon atmosphere. The solvent was evaporated under reduced pressure. The pure product was isolated by column chromatography over silica (CHCl$_3$) as slightly yellow powder (85 mg, 77%). ^{1}H NMR (CDCl$_3$, 300 MHz) δ 8.80 (s, 1H), 8.65 (s, 1H), 8.32–8.25 (m, 3H), 7.98–7.96. (m, 1H), 7.85–7.82 (m, 2H), 7.74–7.71 (m, 2H), 7.61–7.47 (m, 3H). ^{13}C NMR (CDCl$_3$, 75 MHz) δ 147.3, 143.3, 139.6, 136.9, 132.4, 129.9, 129.1, 123.7, 120.5, 91.2, 91.1 (some carbon signals are missing due to the low solubility of the compound). ESI-HRMS calcd for C$_{21}$H$_{13}$N$_5$O$_2$Na ([M + Na]$^+$) 390.0961, found 390.0940.

2-(1-(4-Bromophenyl)-1*H*-[1,2,3]triazol-4-yl)pyridine (13). Sodium azide (480 mg, 7.5 mmol) and anhydrous CuSO$_4$ (80 mg, 0.5 mmol) were dissolved in abs methanol (40 mL). (4-Bromophenyl)boronic acid (1 g, 5 mmol) was added to the brown solution and the reaction mixture was stirred for 48 h at room temperature. The conversion was controlled by TLC on silica (ethyl acetate). Sodium ascorbate (400 mg, 2 mmol, in 1 mL of water), 2-ethynylpyridine (515 mg, 5 mmol), and water (5 mL) were added. The reaction was stirred for 5 days at 40 °C. After that, an excess of water was added to the reaction mixture and the precipitate was filtered off. The filtrate was cautiously extracted with CHCl$_3$ and the organic extract was combined with the precipitate. The CHCl$_3$ solution was dried over NaSO$_4$ and filtered and the solvent was evaporated. Subsequent recrystallization from ethanol provided the pure product as colorless crystals (905 mg, 61%). ^{1}H NMR (CDCl$_3$, 300 MHz) δ 8.62–8.60 (m, 1H), 8.59 (s, 1H), 8.24–8.21 (m, 1H), 7.83–7.80 (m, 1H), 7.75–7.67 (m, 4H), 7.29–7.26 (m, 1H). ^{13}C NMR (CDCl$_3$, 75 MHz) δ 149.5, 137.0, 133.0, 123.2, 121.8, 120.5, 119.8. Anal. Calcd for C$_{13}$H$_9$BrN$_4$: C 51.85, H 3.01, N 18.60. Found: C 51.76, H 3.09, N 18.69.

2-(1-(4-Ethynylphenyl)-1*H*-[1,2,3]triazol-4-yl)pyridine (14). 2-(1-(4-Bromophenyl)-1*H*-[1,2,3]triazol-4-yl)pyridine (**13**, 600 mg, 2 mmol), trimethylsilylacetylene (0.3 mL, 2.05 mmol), tetrakis(triphenylphosphine)palladium(0) (95 mg, 0.08 mmol) and CuI (18 mg, 0.08 mmol) were dissolved in a degassed NEt$_3$/THF mixture (2:1 ratio, 10 mL) and the reaction mixture was stirred for 24 h at 40 °C under argon atmosphere. The solution was evaporated under reduced pressure. The trimethylsilyl-protected product was isolated by column chromatography over silica (CHCl$_3$). The product was dissolved in a MeOH/THF solvent mixture (2:1 ratio, 30 mL) and treated with aq NaOH (200 mg of NaOH in 3 mL of water). After stirring overnight under an argon atmosphere the final product was purified by column chromatography over silica (CHCl$_3$) and obtained as white powder (340 mg, 69%). ^{1}H NMR (CDCl$_3$, 300 MHz) δ 8.63–8.60 (m, 2H), 8.23–8.20 (m, 1H), 7.84–7.78 (m, 3H), 7.67–7.63 (m, 2H), 7.26–7.21 (m, 1H), 3.19 (s, 1H). ^{13}C NMR (CDCl$_3$, 75 MHz) δ 149.7, 149.5, 136.9, 133.5, 123.1, 122.8, 120.4, 120.0, 119.6, 82.2, 79.0. Anal. Calcd for C$_{15}$H$_{10}$N$_4$: C 73.16, H 4.09, N 22.75. Found: C 73.34, H 4.12, N 23.04.

2-(1-(4-((4-Nitrophenyl)ethynyl)phenyl)-1*H*-[1,2,3]triazol-4-yl)pyridine (15). 2-(1-(4-Ethynylphenyl)-1*H*-[1,2,3]triazol-4-yl)pyridine (**14**, 65 mg, 0.26 mmol), 1-iodo-4-nitrobenzene (68 mg,

0.27 mmol), tetrakis(triphenylphosphine)palladium(0) (16 mg, 0.006 mmol), and CuI (3 mg, 0.006 mmol) were dissolved in a degassed NEt$_3$/THF mixture (10:1 ratio, 25 mL) and the solution was stirred for 24 h at 50 °C under argon atmosphere. The solvents were evaporated under reduced pressure and the pure product was obtained by crystallization from chloroform at 5 °C (48 mg, 50%). ^{1}H NMR (CDCl$_3$, 300 MHz) δ 8.66−8.62 (m, 2H), 8.25−8.22 (m, 3H), 7.88−7.70 (m, 7H), 7.30−7.26 (m, 1H). ^{13}C NMR (CDCl$_3$, 75 MHz) δ 147.3, 133.4, 132.4, 129.6, 123.7, 122.8, 120.2, 119.6, 93.1 (some carbon signals are missing due to the low solubility of the compound). ESI-TOF MS: m/z 368.12 ([M + H]$^+$). Anal. Calcd for C$_{21}$H$_{13}$N$_5$O$_2$: C 68.66, H 3.57, N 19.06. Found: C 68.32, H 3.74, N 19.31.

General Procedure for Complexing the (1H-1,2,3-Triazole)-pyridine Ligand to Ru(dmbpy)$_2$Cl$_2$. *cis*-Dichlorobis(4,4′-dimethyl-2,2′-bipyridine)ruthenium(II)[11] (43 mg, 0.08 mmol) and the respective 1H-[1,2,3]triazole ligand (0.08 mmol) were suspended in degassed ethanol (8 mL). After heating under microwave irradiation at 125 °C for 2 h, the red solution was treated with a 10-fold excess of NH$_4$PF$_6$ and subsequently stirred until precipitation occurred (10 min to 2 h). The colored precipitate was filtered off and purified by washing twice with ethanol and diethyl ether providing the pure product. In the cases where the ^{1}H NMR spectrum indicated any impurities, the compound was further purified by recrystallization from ethanol.

Bis(4,4′-dimethyl-2,2′-bipyridine)-{2-(1-decyl-1H-[1,2,3]tri-azol-4-yl)-5-((4(hexyloxy)phenyl)ethynyl)pyridine}ruthenium(II) Hexafluorophosphate (16a). According to the above standing general procedure *cis*-dichlorobis(4,4′-dimethyl-2,2′-bipyridine)-ruthenium(II) (30 mg, 0.056 mmol) and 2-(1-decyl-1H-[1,2,3]-triazol-4-yl)-5-((4-(hexyloxy)phenyl)ethynyl)pyridine (**5**, 27 mg, 0.056 mmol) were reacted to yield the complex as an orange powder after washing twice with ethanol and diethyl ether (55 mg, 81%). ^{1}H NMR (CD$_3$CN, 300 MHz) δ 8.68 (s, 1H), 8.38 (s, 2H), 8.31 (s, 1H), 8.28 (s, 1H), 8.10−8.0 (m, 2H), 7.73−7.61 (m, 4H), 7.50 (d, J = 5.8 Hz, 1H), 7.43−7.38 (m, 2H), 7.28−7.22 (m, 3H), 7.17−7.14 (m, 1H), 6.94−6.87 (m, 2H), 4.34 (t, J = 7.0 Hz, 2H), 4.0 (t, J = 6.5 Hz, 2H), 2.56−2.52 (m, 12H), 1.95−1.92 (m, 4H), 1.83−1.69 (m, 4H), 1.47−1.08 (m, 20H), 0.93−0.86 (m, 6H). ^{13}C NMR (CD$_3$CN, 75 MHz) δ 161.3, 158.1, 157.8, 157.7, 157.5, 153.8, 152.2, 152.1, 152.0, 151.9, 151.21, 151.2, 151.1, 150.9, 150.6, 148.1, 140.5, 134.2, 129.2, 129.0, 128.4, 126.6, 125.9, 125.8, 125.4, 125.0, 123.3, 122.9, 115.8, 113.9, 96.6, 83.8, 69.1, 53.0, 32.6, 32.2, 30.1, 30.0, 29.9, 29.7, 29.3, 26.6, 26.3, 23.3, 23.2, 21.22, 21.2, 21.1, 14.3, 14.2. ESI-TOF MS m/z 1101.40 ([M − PF$_6$]$^+$), 478.22 ([M − 2PF$_6$]$^{2+}$). ESI-HRMS calcd for C$_{55}$H$_{66}$N$_8$ORu [M − 2PF$_6$]$^{2+}$ 478.2203, found 478.2199.

Bis(4,4′-dimethyl-2,2′-bipyridine)-{2-(1-decyl-1H-[1,2,3]triazol-4-yl)-5-((4-nitrophenyl)ethynyl)pyridine}ruthenium(II) Hexafluorophosphate (16b). According to the above standing general procedure *cis*-dichlorobis(4,4′-dimethyl-2,2′-bipyridine)ruthenium(II) (35 mg, 0.065 mmol) and 2-(1-decyl-1H-[1,2,3]triazol-4-yl)-5-((4-nitrophenyl)ethynyl)pyridine (**10a**, 28 mg, 0.065 mmol) were reacted to yield the pure complex as an orange powder after washing twice with ethanol and diethyl ether (68 mg, 88%). ^{1}H NMR ((CD$_3$)$_2$CO, 300 MHz) δ 9.23 (s, 1H), 8.67−8.60 (m, 4H), 8.42−8.39 (m, 1H), 8.30−8.25 (m, 3H), 8.12−8.08 (m, 2H), 7.96 (d, 1H), 7.87 (d, 1H), 7.78−7.70 (m, 3H), 7.44−7.32 (m, 4H), 4.52 (t, J = 7.1 Hz, 2H), 2.58−2.52 (m, 12H), 2.05−2.01 (m, 2H), 1.89−1.79 (m, 2H), 1.25−1.07 (m, 12H), 0.87−0.81 (m, 3H). ^{13}C NMR ((CD$_3$)$_2$CO, 75 MHz) δ 158.1, 158.0, 157.8, 154.5, 152.4, 152.21, 152.2, 151.2, 151.1, 148.9, 148.2, 141.4, 133.6, 129.4, 129.0, 128.7, 126.0, 125.5, 125.2, 124.7, 123.1, 121.9, 95.6, 89.3, 52.1, 32.6, 26.7, 23.3, 21.2, 14.3. ESI-TOF MS m/z 1046.3 ([M − PF$_6$]$^+$), 450.67 ([M − 2PF$_6$]$^{2+}$). ESI-HRMS calcd for C$_{49}$H$_{53}$N$_9$O$_2$Ru ([M − 2PF$_6$]$^{2+}$): 450.6684, found 450.6685.

Bis(4,4′-dimethyl-2,2′-bipyridine)-{2-(1-decyl-1H-[1,2,3]tri-azol-4-yl)-5-((4-(trifluoromethyl)phenyl)ethynyl)pyridine}ruthenium-(II) Hexafluorophosphate (16c). According to the above standing general procedure *cis*-dichlorobis(4,4′-dimethyl-2,2′-bipyridine)-ruthenium(II) (30 mg, 0.056 mmol) and 2-(1-decyl-1H-[1,2,3]tri-azol-4-yl)-5-((4-(trifluoromethyl)phenyl)ethynyl)pyridine (**10c**, 25 mg, 0.056 mmol) were reacted to yield the pure complex as red powder after recrystallization from ethanol (32 mg, 48%). ^{1}H NMR (CD$_3$CN, 300 MHz) δ 8.71 (s, 1H), 8.38 (s, 2H), 8.31−8.27 (m, 2H), 8.11−8.08 (m, 2H), 7.79−7.60 (m, 8H), 7.49−7.46 (m, 1H), 7.28−7.23 (m, 3H), 7.18−7.16 (m, 1H), 4.35 (t, J = 7.0 Hz, 2H), 2.56−2.51 (m, 12H), 1.80−1.72 (m, 2H), 1.37−1.07 (m, 14H), 0.89 (t, J = 6.7 Hz, 3H). ^{13}C NMR (CD$_3$CN, 75 MHz) δ 157.2, 156.9, 156.7, 156.6, 153.4, 151.3, 151.2, 151.1, 151.0, 150.7, 150.3, 150.3, 150.2, 150.0, 147.1, 140.1, 132.2, 128.2, 128.0, 127.5, 126.0, 125.7, 125.6, 125.0, 124.9, 124.5, 124.1, 122.1, 121.3, 93.2, 86.1, 52.1, 31.6, 29.2, 29.2, 29.1, 29.0, 28.4, 25.6, 22.4, 20.4, 20.3, 20.2, 13.4. ESI-TOF MS m/z 1069.30 ([M − PF$_6$]$^+$), 462.17 ([M − 2PF$_6$]$^{2+}$). ESI-HRMS calcd for C$_{50}$H$_{53}$F$_9$N$_8$PRu ([M − PF$_6$]$^+$) 1069.3025, found 1069.2993.

Bis(4,4′-dimethyl-2,2′-bipyridine)-{2-(1-decyl-1H-[1,2,3]tri-azol-4-yl)-5-((2-nitrophenyl)ethynyl)pyridine}ruthenium(II) Hexafluorophosphate (16d). According to the above standing general procedure *cis*-dichlorobis(4,4′-dimethyl-2,2′-bipyridine)ruthenium-(II) (30 mg, 0.056 mmol) and 2-(1-decyl-1H-[1,2,3]triazol-4-yl)-5-((2-nitrophenyl)ethynyl)pyridine (**10b**, 24 mg, 0.056 mmol) were reacted to yield the pure complex as red powder after washing twice with ethanol and diethyl ether (59 mg, 90%). ^{1}H NMR (CD$_3$CN, 300 MHz) δ 8.71 (s, 1H), 8.38−8.29 (m, 4H), 8.13−8.09 (m, 3H), 7.74−7.53 (m, 8H), 7.27−7.23 (m, 3H), 7.17−7.15 (m, 1H), 4.35 (t, J = 7.0 Hz, 2H), 2.58−2.52 (m, 12H), 1.80−1.72 (m, 2H), 1.37−1.07 (m, 14H), 0.89 (t, J = 6.7 Hz, 3H). ^{13}C NMR (CD$_3$-CN, 75 MHz) δ 158.1, 157.8, 157.7, 157.5, 154.5, 152.2, 152.2, 152.0, 151.8, 151.6, 151.3, 151.2, 150.9, 147.9, 140.5, 135.5, 134.6, 131.5, 129.2, 129.0, 128.4, 127.0, 126.0, 125.9, 125.8, 125.4, 125.1, 123.0, 122.1, 91.4, 91.2, 53.1, 32.6, 30.1, 30.1, 30.0, 29.9, 29.3, 26.6, 23.3, 21.3, 21.2, 21.1, 14.3. ESI-TOF MS m/z 1046.30 ([M − PF$_6$]$^+$), 450.67 ([M − 2PF$_6$]$^{2+}$). ESI-HRMS calcd for C$_{49}$H$_{53}$F$_6$N$_9$O$_2$PRu ([M − PF$_6$]$^+$) 1046.3002, found 1046.2997.

Bis(4,4′-dimethyl-2,2′-bipyridine)-{5-((4-phenyl)ethynyl)-2-(1-phenyl-1H-[1,2,3]triazol-4-yl)pyridine}ruthenium(II) Hexafluorophosphate (16e). According to the above-mentioned general procedure *cis*-dichlorobis(4,4′-dimethyl-2,2′-bipyridine)ruthenium(II) (30 mg, 0.056 mmol) and 5-((4-phenyl)ethynyl)-2-(1-phenyl-1H-[1,2,3]triazol-4-yl)pyridine (**10d**, 23 mg, 0.056 mmol) were reacted to yield the pure complex as red powder after washing twice with ethanol and diethyl ether (48 mg, 75%). ^{1}H NMR (CD$_3$CN, 300 MHz) δ 8.69 (s, 1H), 8.37−8.27 (m, 4H), 8.11−8.05 (m, 2H), 7.75−7.72 (m, 2H), 7.66−7.62 (m, 2H), 7.50−7.39 (m, 6H), 7.27−7.24 (m, 3H), 7.18−7.16 (m, 1H), 4.34 (t, J = 7.0 Hz, 2H), 2.56−2.51 (m, 12H), 1.79−1.71 (m, 2H), 1.37−1.06 (m, 14H), 0.89 (t, J = 6.7 Hz, 3H). ^{13}C NMR (CD$_3$CN, 75 MHz) δ 157.2, 156.9, 156.7, 156.6, 153.2, 151.3, 151.2, 151.1, 151.0, 150.3, 150.3, 150.2, 150.2, 150.0, 147.1, 139.9, 131.6, 129.7, 128.8, 128.2, 128.0, 127.5, 125.8, 125.0, 124.9, 124.5, 124.1, 122.0, 121.9, 121.4, 95.0, 83.9, 52.1, 31.6, 29.2, 29.1, 29.0, 28.4, 25.6, 22.4, 20.3, 20.2, 13.4. ESI-TOF MS m/z 1001.32 ([M − PF$_6$]$^+$), 428.18 ([M − 2PF$_6$]$^{2+}$). ESI-HRMS calcd for C$_{49}$H$_{54}$F$_6$N$_8$PRu [M − PF$_6$]$^+$ 1001.3151, found 1001.3168.

Bis(4,4′-dimethyl-2,2′-bipyridine)-{5-((4-nitrophenyl)ethynyl)-2-(1-phenyl-1H-[1,2,3]triazol-4-yl)pyridine}ruthenium(II) Hexafluorophosphate (17). According to the above standing general procedure Ru(dmbpy)$_2$Cl$_2$ (35 mg, 0.065 mmol) and 5-((4-nitrophenyl)ethynyl)-2-(1-phenyl-1H-[1,2,3]triazol-4-yl)pyridine (**12**, 24 mg, 0.065 mmol) were reacted to yield the pure complex as red powder after washing twice with ethanol and diethyl ether (45 mg, 63%). ^{1}H NMR (CD$_3$CN, 300 MHz) δ 9.24 (s, 1H), 8.39 (s, 2H), 8.33−8.18 (m, 6H), 7.86 (s, 1H), 7.79−7.76 (m, 2H),

7.71−7.53 (m, 9H), 7.29−7.25 (m, 3H), 7.17 (m, 1H), 2.56−2.53 (m, 12H). ^{13}C NMR (CD$_3$CN, 75 MHz) δ 157.1, 156.8, 156.7, 156.5, 153.7, 151.5, 151.4, 151.0, 150.9, 150.5, 150.5, 150.4, 150.4, 150.2, 148.0, 140.4, 136.1, 132.7, 130.3, 130.1, 128.3, 128.2, 128.0, 127.5, 125.0, 124.9, 124.6, 124.2, 123.9, 122.2, 121.4, 120.7, 92.9, 88.2, 20.3, 20.3, 20.2. ESI-TOF MS m/z 982.17 ([M − PF$_6$]$^+$). ESI-HRMS calcd for C$_{45}$H$_{37}$F$_6$N$_9$O$_2$PRu ([M − PF$_6$]$^+$) 982.1750, found 982.1776.

Bis(4,4′-dimethyl-2,2′-bipyridine)-{2-(1-(4-((4-nitrophenyl)-ethynyl)phenyl)-1*H*-[1,2,3]triazol-4-yl)pyridine}ruthenium(II) Hexa-fluorophosphate (18). According to the above standing general procedure Ru(dmbpy)$_2$Cl$_2$ (25 mg, 0.046 mmol) and 2-(1-(4-((4-nitrophenyl)ethynyl)phenyl)-1*H*-[1,2,3]triazol-4-yl)pyridine (**15**, 17 mg, 0.046 mmol) were reacted 2.5 h to yield the pure complex as red powder after washing twice with ethanol and diethyl ether (40 mg, 77%). ^{1}H NMR (CD$_3$CN, 300 MHz) δ 9.25 (s, 1H), 8.38−8.32 (m, 4H), 8.25−8.21 (m, 2H), 8.17−8.15 (m, 1H), 8.03−8.0 (m, 1H), 7.83−7.73 (m, 7H), 7.71−7.58 (m, 4H), 7.36−7.19 (m, 5H), 2.55−2.51 (m, 12H). ^{13}C NMR (CD$_3$CN, 75 MHz) δ 157.2, 156.8, 156.8, 156.5, 151.7, 151.3, 151.1, 151.1, 150.8, 150.6, 150.4, 150.3, 150.1, 148.7, 147.6, 138.1, 136.1, 133.4, 132.5, 129.0, 128.3, 128.2, 127.5, 126.2, 124.9, 124.8, 124.6, 124.2, 123.9, 123.8, 123.4, 122.7, 120.8, 92.1, 89.4, 20.3, 20.3. ESI-TOF MS m/z 982.17 ([M − PF$_6$]$^+$). ESI-HRMS calcd for C$_{45}$H$_{37}$F$_6$N$_9$O$_2$PRu ([M − PF$_6$]$^+$) 982.1750, found 982.1759.

Supporting Information Available: UV−vis absorption and emission spectra for the ligands and corresponding ruthenium complexes, crystallographic data for **17**, computational details of **16a** and **16b** (Cartesian coordinates and total energies), and ^{1}H and ^{13}C NMR spectra of all new compounds. This material is available free of charge via the Internet at http://pubs.acs.org.